Differential expression analysis of PMA and 1,25$(OH)_2D_3$-induced monocyte-to-macrophage differentiation in THP-1 cells

by

Kelda Chloe Perumal

(1603690)

Dissertation

Submitted in fulfilment of the requirements for the degree

Master of Science

in

Molecular and Cell Biology

in the Faculty of Science, University of the Witwatersrand, Johannesburg, South Africa

Supervisor: Dr N Gentle

Co-supervisor: Dr V Meyer

September 2023

Declaration

I, Kelda Chloe Perumal (1603690), am a student registered for the degree of Master of Science in the academic year 2023.

I hereby declare the following:

- I am aware that plagiarism (the use of someone else's work without their permission and/or without acknowledging the original source) is wrong.
- I confirm that the research dissertation submitted for assessment for the above degree is my own unaided work except where explicitly indicated otherwise and acknowledged.
- I have followed the required conventions in referencing the thoughts and ideas of others.
- I understand that the University of the Witwatersrand may take disciplinary action against me if there is a belief that this is not my own unaided work or that I have failed to acknowledge the source of the ideas or words in my writing.

Signature 

03 September 2023

Acknowledgments

To my supervisors. Dr Gentle, thank you for your continuous support, guidance and most-especially, patience throughout this journey. I have learned so much from you. None of this would have been possible without you. Thank you for inspiring me. I will forever be grateful. Dr Meyer, thank you for holding down the forte when you needed to and even when you didn't. I appreciate you and all your help, guidance and kindness along the way.

To the University of the Witwatersrand for awarding me with the Post Graduate Merit Award as well as the National Research Foundation, for allowing me the opportunity to pursue this research, I would like to express my deepest appreciation.

To my parents, the reason for my existence. Thank you for always surrounding me with nothing but love and always encouraging me to do my best. It's all for you. I hope that I make you proud. To my brother, Em, thank you for your love and support throughout this, it didn't go unnoticed. I appreciate you.

To my lab colleagues. Darisia, your friendship is one I will treasure for a lifetime. Thank you for making everything a little more bearable all the time. Thank you for always being willing to help and for helping as if every problem is your own. I appreciate you. Asavela, we started this journey together and I am so grateful for you and your kindness. We did it! Yi, thank you for all your help and for always making us laugh.

Research Outputs

Presentations

- Perumal, K., Meyer, V., Gentle, N. Differences and commonalities induced by PMA and 1,25(OH)2D3 in THP-1 cells during monocyte-to-macrophage differentiation. SASBI/SAGS Student Symposium, September 2021
- Perumal, K., Meyer, V., Gentle, N. Differences and commonalities induced by PMA and 1,25(OH)2D3 in THP-1 cells during monocyte-to-macrophage differentiation. MBRT Virtual Postgraduate Research Day, December 2021
- Perumal, K., Meyer, V., Gentle, N. Differences and commonalities induced by PMA and 1,25(OH)2D3 in THP-1 cells during monocyte-to-macrophage differentiation. South African Genetics Society & South African Society for Bioinformatics Joint BIO22 Conference, Stellenbosch, April 2022

Table of Contents

List of Abbreviations

bp	Base Pairs
BP	Biological Process
CC	Cellular Component
cDNA	Complementary Deoxyribonucleic Acid
cMoP	Common Monocyte Progenitor
CMP	Common Myeloid Progenitor
CSF-1	Colony Stimulating Factor 1
CSF-1R	Colony Stimulating Factor 1 Receptor
DAMP	Damage-Associated Molecular Patterns
DC	Dendritic Cell
DEG	Differentially Expressed Genes
DGE	Differential Gene Expression
ENA	European Nucleotide Archive
FDR	False Discovery Rate
GLM	General Linear Model
GMP	Granulocyte-macrophage Progenitor
GO	Gene Ontology
HCMV	Human Cytomegalovirus
HSC	Hematopoietic Stem Cell
IFN-Y	Interferon Gamma
KEGG	Kyoto Encyclopaedia of Genes and Genomes
KLF4	Kruppel-like Factor 4
LPS	Lipopolysaccharide
M-CSF	Macrophage Colony Stimulating Factor
MAPK	Mitogen Activated Protein Kinases
MDP	Macrophage Dendritic Cell Progenitor
MEP	Megakaryocyte-Erythroid Progenitor
MeSH	Medical Subject Headings
MF	Molecular Function

mRNA	Messenger Ribonucleic Acid
NGS	Next Generation Sequencing
NK	Natural Killer
ORA	Over Representation Analysis
PAMP	Pathogen-Associated Molecular Pattern
PCA	Principal Components Analysis
PMA	phorbol 12-myristate 13-acetate
PRR	Pathogen Recognition Receptor
RNA	Ribonucleic Acid
RNA-seq	Ribonucleic Acid Sequencing
RXR	Retinoid X Receptor
TLR	Toll-like Receptor
TNF	Tumour Necrosis Factor
TPM	Transcripts per Million
TRM	Tissue Resident Macrophage
VD3	Vitamin D_3/1,25 dihydroxyvitamin D_3/1,25$(OH)_2D_3$
VDR	Vitamin D_3 Receptor
VDRE	Vitamin D Response Element

List of Figures

List of Tables

Abstract

The process of monocyte-to-macrophage differentiation is studied *in vitro* through the use of promonocytic model cell lines, such as the THP-1 cell line, where commonly used differentiation inducing agents include phorbol-12-myristate-13-acetate (PMA) and the active metabolite of vitamin D_3, ($1,25(OH)_2D_3$; VD_3). While both induce differentiation, differences in their mechanisms of action, as well as how the end states of the differentiation process differ, are not well understood. Therefore, this study used computational approaches to compare the effects of PMA and VD_3 on the differentiation of monocytes into macrophages, using the promonocytic THP-1 cell line. Through the use of RNA-sequencing, gene expression was quantified in differentiated and undifferentiated THP-1 cells, treated with both PMA and VD_3. Differential gene expression analysis was performed to determine genes that were differentially expressed as a result of either treatment relative to the untreated cells. This was followed by over-representation analysis to determine the pathways and processes in which the differentially expressed genes (DEGs) were involved. PMA treatment (3 989 DEGs) resulted in more changes in expression relative to VD_3 treatment, where only 384 genes were found to be differentially expressed in response to treatment with VD_3. Only *TFE3*, *KIT* and *TRIB1* were observed to be crucial to the process of differentiation, irrespective of treatment. Apart from this, the treatments were observed to largely involve different biological pathways, resulting in cells that were phenotypically distinct from each other at the transcriptional level. This included changes observed in the expression of genes encoding transcription factors known to be involved in the differentiation process, such as *CEBPA, GATA2, IRF8* and *PU.1*, as well as those encoding surface markers representative of monocytes and macrophages, such as *CD14*, *CD64* and *CD11b*. The expression patterns observed here indicate that, at least at the concentrations and time points included in this study, PMA and VD_3 induce macrophage-like cells that are at different stages of differentiation and are not comparable to either each other or primary macrophages. Furthermore, key differences observed in the expression of genes encoding pathogen recognition receptors and cytokines suggest that which differentiation-inducing agent is used may have important implications for these cells' capacity to recognise pathogens and produce cytokines. The findings of this study therefore emphasise that it is crucial to carefully consider the choice of differentiation-inducing agent when using THP-1 cells as an experimental system for studying monocyte-to-macrophage differentiation.

Chapter 1: Literature Review

1.1. Innate Immunity

The innate immune system establishes the earliest response to a pathogen's invasion of a cell or tissue. Innate immunity occurs within minutes to hours of initial infection and involves both physical barriers and molecular mechanisms (Murphy and Weaver, 2016). The cells constituting the innate immune system have the ability to recognise and distinguish between host (self) and pathogenic (non-self) material. These cells are derived from one of two haematopoietic lineages, namely the lymphoid and the myeloid lineages (Figure 1.1). Lymphoid cells include natural killer (NK) cells, B cells, and T lymphocytes. The myeloid lineage includes neutrophils, eosinophils, mast cells, monocytes, macrophages, and dendritic cells (DCs) - all of which are involved in the innate immune response.

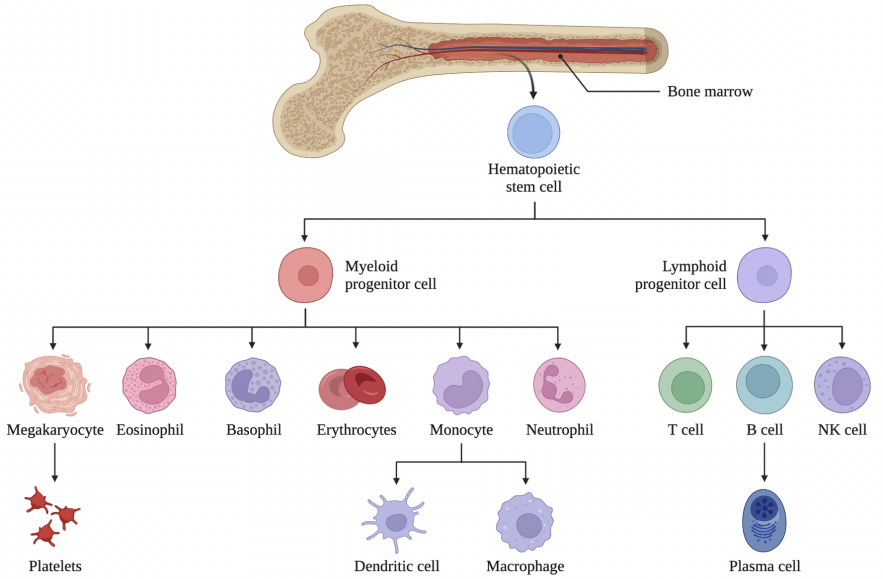

Figure 1.1: Immune cell lineages. Hematopoietic stem cells (HSCs) are derived from the bone marrow. They progressively differentiate into pluripotent stem cells that produce the myeloid and lymphoid lineages of leukocytes. Myeloid progenitors give rise to common innate immune cells such as eosinophils, neutrophils, basophils, and monocytes. Monocytes further differentiate into dendritic cells (DCs) and macrophages. Myeloid progenitors further give rise to megakaryocytes (platelets) and erythrocytes (red blood cells). The lymphoid arm of the hierarchy includes natural killer (NK) cells, as well as B and T lymphocytes (Image obtained from www.biorender.com).

Innate immune cells possess pathogen recognition receptors (PRRs), which enable the innate immune response to discern between self and non-self (Janeway and Medzhitov, 2002). PRRs are germline encoded receptors, found both on the surface of immune cells and within the cells (Akira *et al.*, 2006), that recognise pathogen-associated molecular patterns (PAMPs). Different PRRs recognise different PAMPs, and in turn induce different signalling pathways, in an attempt to produce an anti-pathogenic response. Different types of PRRs that are involved in PAMP sensing in innate immune cells are the toll-like receptors (Liu *et al.*, 2007; Medzhitov *et al.*, 1997), RIG 1-like receptors (Yoneyama *et al.*, 2004) and NOD-like receptors (Girardin *et al.*, 2003; Martinon and Tschopp, 2004).

1.2. The Hematopoietic Cell Lineage

The hematopoietic system is a hierarchical system that is responsible for the production of the innate and adaptive immune cells (Figure 1.1). In particular, hematopoietic stem cells (HSCs) are cells that are capable of differentiating into different types of myeloid and lymphoid blood cells. HSCs are found in the bone marrow, as well as in peripheral blood (Lee and Hong, 2019). The ability that these cells possess to differentiate into different cell types, as well as their ability to initiate and sustain the production of mature blood cells makes them multipotent. In addition to multipotency, other properties of HSCs include self-renewal and quiescence. The process of differentiation of a HSC to a mature blood cell involves many intermediate progenitor cells.

1.3. The Myeloid Lineage

The myeloid lineage (Figure 1.2) comprises cells originating from the progressive differentiation of the HSC into the common myeloid progenitor (CMP), followed by the granulocyte-macrophage progenitor (GMP). Granulocytes are the most abundant myeloid cell type found in the bloodstream, and they can be further classified into neutrophils, eosinophils, and basophils. All granulocytes originate from the GMP, which differentiates into the relevant lineage-committed progenitors for eosinophils and basophils/mast cells. In adults, neutrophils are the most abundant granulocytes found in circulation. Neutrophils circulate until recruited to a site of infection/injury by tissue-resident macrophages (De Kleer *et al.*, 2014). Monocytes, macrophages, and DCs develop through the monocyte/macrophage and DC progenitor (MDP).

MDPs do not have the ability to give rise to granulocytes, and therefore, through the common monocyte progenitor (cMoP; Hettinger *et al.*, 2013), they are restricted to monocytes and their derivatives (Naik *et al.*, 2006; De Kleer *et al.*, 2014).

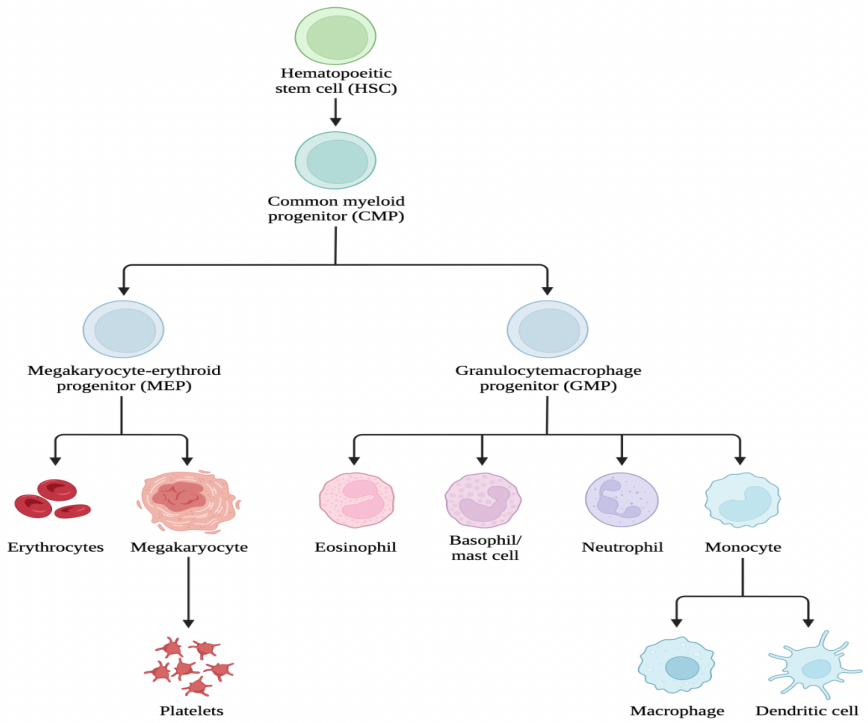

Figure 1.2: The myeloid lineage. The common myeloid progenitor (CMP) is derived from the HSC. The CMP then gives rise to a megakaryocyte-erythroid progenitor (MEP), which further differentiates into erythrocytes (red blood cells) and megakaryocytes (platelets). The CMP also gives rise to a granulocyte-macrophage progenitor (GMP), which further differentiates into eosinophils, basophils, neutrophils and monocytes. Eosinophils, basophils, and neutrophils are known as granulocytes and are found in circulation. Monocytes, upon entering tissues, can undergo further differentiation into macrophages and dendritic cells (DCs). (Image obtained from and edited in www.biorender.com)

1.4. Macrophages

Present in every tissue of the body, macrophages are the first cells recruited to a site of infection (Murray and Wynn, 2011). Elie Metchnikoff, a developmental embryologist, coined the term "macrophage" in the late 19th century (Metchnikoff, 1883). He described an immune cell population devoted to phagocytosis, the process by which cells consume and destroy foreign particles such as bacteria (Metchnikoff, 1891). Since their discovery, macrophages and their

functions have been extensively studied (Jenkins *et al.*, 2013; Misharin *et al.*, 2013; Yáñez *et al.*, 2013; Bertani *et al.*, 2017; Atri *et al.*, 2018; Huang *et al.*, 2019). Macrophages are often identified using common cell surface protein markers that can be assessed using flow cytometry; including cluster of differentiation (CD)11c, CD64, CD14, CD16, CD11b, CD80, CD206 (Misharin *et al.*, 2013; Bertani *et al.*, 2017).

1.4.1 Tissue-Resident Macrophages

Populations of tissue-resident macrophages comprise both embryonically-derived and bone marrow-derived macrophages (Figure 1.3; Sieweke and Allen, 2013). The latter develop through the recruitment and subsequent differentiation of circulating monocytes. The functionality of tissue-resident macrophages is dependent on ontogeny, the local milieu, inflammation, and the duration in which the cell spends within the tissue (Blériot *et al.*, 2020). In addition to their role during infection, tissue-resident and monocyte-derived macrophages also have an important role to play during the steady-state, in terms of homeostasis, where they eliminate apoptotic cells, proteins, and phospholipids from the local microenvironment and either eliminate or respond to toxins and pathogens. Tissue-resident macrophages can sustain themselves through local proliferation without the assistance of monocyte-derived macrophages (Davies *et al.*, 2013; Blériot *et al.*, 2020).

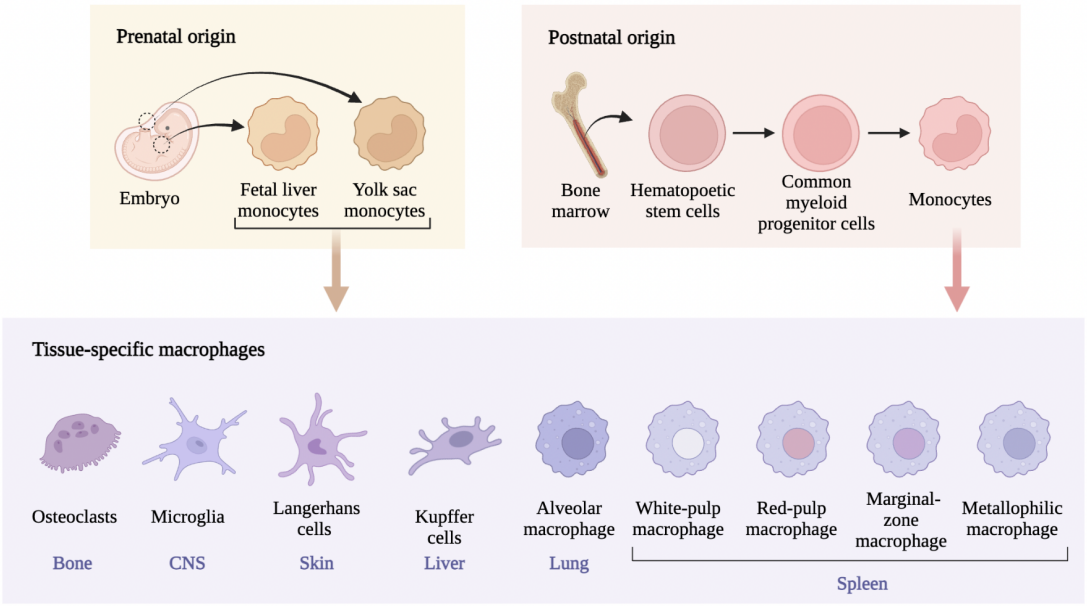

Figure 1.3: Ontogeny of tissue-resident macrophages (TRMs). TRMs can be of prenatal origin, where differentiation of foetal liver monocytes and yolk sac monocytes are responsible for the differentiation and population of TRMs. Alternatively, TRMs can be of post-natal origin, where circulating monocytes differentiate and populate the tissues. TRMs adopt different names according to the tissue in which they reside (Image obtained from www.biorender.com).

1.4.2 The Role of Macrophages in the Maintenance of Homeostasis

While macrophages play an essential role during infection, they are also responsible for the removal of dead cellular and tissue debris from the body (Wynn *et al.*, 2013; Mosser *et al.*, 2020), which, if allowed to accumulate, would prevent regular organ functionality. Mosser *et al.* (2020) proposed the term "transducer" when referring to macrophages in the steady-state. Macrophages are found in tissues such as the epidermis, cornea, and joint interiors, all of which lack blood vessels. In this way, macrophages are essential cells that serve as 'transducers' by obtaining information from tissues and translating it into signals that induce a response. These responses are generally associated with the physiological processes that are vital for the organ's daily function (Mosser *et al.*, 2020).

1.4.3 The Role of Macrophages During Infection

Being tissue-resident allows macrophages to be among the first innate immune cells to interact with invading pathogens. Upon this interaction, macrophages perform two main functions:

effector functions and sentinel functions. As effector cells, macrophages phagocytose pathogens and infected and dying cells, up-regulate antimicrobial peptide production, and induce cell death (Murphy and Weaver, 2016; Sheu and Hoffmann, 2022). By secreting cytokines, chemokines, and growth factors, and presenting antigens to adaptive immune cells, macrophages serve as sentinels, initiating and coordinating local or systemic immune activation. The release of chemoattractants by TRMs initiates the extravasation of circulating monocytes into the tissue (Sheu and Hoffmann, 2022). Here the monocytes interact with PAMPs or damage-associated molecular patterns (DAMPs), upon which they rapidly differentiate into macrophages (Murphy and Weaver, 2016; Sheu and Hoffmann, 2022). This differentiation allows more cells to contribute to effector and sentinel functions at a site of infection.

1.4.4 Macrophage Polarisation

Macrophages are polarised in response to environmental changes (i.e., cytokines and signalling pathways), resulting in the formation of distinct, active macrophage subtypes: M1 and M2 macrophages. It has long been recognized that M1 macrophages refer to those that are classically activated, while M2 macrophages constitute alternatively activated macrophages. M2 macrophages can be further classified into M2a, M2b and M2c subsets. These are activated through interleukin (IL)-4 and IL-13 (M2a; Mantovani *et al.*, 2004), immune complexes and toll-like receptor (TLR) ligands (M2b; Mosser, 2003; Mosser and Edwards, 2008), interleukin 10 (IL-10), Glucocorticoids, transforming growth factor beta (TGFβ) (M2c; Mosser, 2003; Zizzo *et al.*, 2012; Zizzo and Cohen, 2013), and TLR and A2R ligands (M2d; Grinberg *et al.*, 2009; Ferrante *et al.*, 2013). The change in cell surface marker expression is a crucial aspect of macrophage polarisation. The M1 macrophage phenotype is known to be induced through interferon gamma (IFN-γ), lipopolysaccharide (LPS), or tumour necrosis factor alpha (TNF-α) stimulation (Mantovani *et al.*, 2004). These macrophages are able to secrete pro-inflammatory cytokines and overexpress cluster of differentiation 80 (CD80), CD86, and CD16/32 (Yunna *et al.*, 2020). While M2 macrophages have higher levels of the chemokines C-C motif chemokine ligand 17 (CCL17) and CCL22, as well as the enzyme arginase-1 (Arg-1), mannose receptor (CD206), and anti-inflammatory factor (IL-10) (Yunna *et al.*, 2020).

1.5 Monocytes

Monocytes are blood cells that make up less than 10% of peripheral leukocytes in humans (van Furth and Sluiter, 1986). It is believed that blood monocytes originate in the adult bone marrow (BM), from a common myeloid progenitor (CMP) that also gives rise to erythrocytes, platelets, dendritic cells, and granulocytes (Akashi *et al.*, 2000; De Kleer *et al.*, 2014; Pietras *et al.*, 2015). Monocytes are discharged into the peripheral circulation after their production. Metchnikoff first observed peripheral blood monocytes in 1905, but until 1925 they were classified together with tissue macrophages and not distinguished as a distinct cell type (Lewis and Lewis, 1925). In the last two decades, sophisticated mouse models, RNA sequencing, confocal microscopy, as well as developments in multi-dimensional analysis of cell surface and intracellular proteins have led to a more complete and accurate understanding of monocyte development (Hettinger *et al.*, 2013; Kurotaki *et al.*, 2013; Yáñez *et al.*, 2013; Kawamura *et al.*, 2017; Roberts *et al.*, 2020).

Using monoclonal antibodies and two-colour flow cytometry, it was possible to identify three distinct human monocyte subsets by as early as 1989, based on CD14 and CD16 expression. The subsets were defined as classical ($CD14^{+}/CD16^{-}$), intermediate ($CD14^{+}/CD16^{+}$) and non-classical ($CD14^{-}/CD16^{+}$) monocytes (Passlick *et al.*, 1989). A more recent study conducted by Thomas *et al*. (2017) found additional markers that, when observed in combination with CD14 and CD16, enhance the identification and distinction of the monocyte subsets. This was made possible through the use of mass cytometry, which enables up to 40 markers to be analysed simultaneously. These markers include CD36, HLA-DR, CD11c and CCR2. By this definition, classical monocytes can be distinguished through $CD14^{+}CD16^{-}$HLA-$DR^{lo}CD11c^{lo}$ expression, intermediate monocytes by $CD14^{+}CD16^{+}CD36^{hi}CCR2^{hi}$HLA-$DR^{hi}CD11c^{hi}$ expression and non-classical monocytes by $CD14^{-}CD16^{+}CD36^{lo}CCR2^{lo}$ expression (Thomas *et al.*, 2017).

1.5.1 The Role of Monocytes in Infection

Upon bacterial infection, monocytes, in response to chemokines, are recruited from the bone marrow in a myeloid differentiation primary response 88 (MYD88) and TLR-dependent manner (Serbina *et al.*, 2003). In addition, monocyte recruitment during *M. tuberculosis* infection has been shown to be CC-chemokine receptor 2 (CCR2)-dependent (Peters *et al.*,

2001). Similarly, in cases of viral infection, CCR2 is responsible for monocyte recruitment into the liver (Salazar-Mather *et al.*, 1998). At a site of infection, monocytes aid in the recruitment of additional innate immune cells, such as NK cells, or alternatively, undergo differentiation into macrophages, for an enhanced innate immune response (Murphy and Weaver, 2016).

1.6 Monocyte-to-Macrophage Differentiation

Monocyte-to-macrophage differentiation is associated with widespread changes in messenger RNA (mRNA) and microRNA (miRNA) levels, which are a consequence of epigenetic changes (histone modifications resulting in changes in chromatin accessibility) (Saeed *et al.*, 2014; Wallner *et al.*, 2016). In addition, colony-stimulating factor 1 (CSF-1), also known as macrophage (M)-CSF, is a crucial factor involved in the process of monocyte-to-macrophage differentiation via the CSF-1 receptor (CSF-1R). However, the CSF-1-mediated signalling pathway by which this differentiation process occurs is poorly understood (Pixley and Stanley, 2004).

It is known that differentiation in the presence of CSF-1 is associated with an increase in cell cycle gene expression (Martinez *et al.*, 2006). Together with cytokines such as IL-4, M-CSF/CSF-1 promotes the growth, differentiation, and proliferation of monocytes and macrophages (Jenkins *et al.*, 2013). In addition, it has also been shown that CSF-1 and IL-34 can both utilise CSF-1R and its associated signalling pathway to trigger monocyte differentiation into macrophages. Differences in signalling and effects of CSF-1 and IL-34 are seen, however, during the polarisation of the differentiated monocytes into M1 or M2 macrophages, where there are distinguishable differences in chemokine/cytokine production (Boulakirba *et al.*, 2018). Furthermore, a number of lineage-determining transcription factors have been found to be involved in this process of differentiation (Table 1.1). One of the key genes is Spi-1 Proto-Oncogene (*SPI1)*, which encodes the PU.1 transcription factor. PU.1 has been associated with different stages of myeloid differentiation (Akashi *et al.*, 2000) and has been found to interact with other transcription factors such as the CCAAT enhancer-binding protein alpha (CEBPα) (Reddy *et al.*, 2002), CEBPβ (Yang *et al.*, 2000), GATA-binding factor 2 (GATA2) (Walsh *et al.*, 2002), and IRF8 (Meraro *et al.*, 1999). PU.1 overexpression activates interferon regulatory factor 8 (IRF8) and kruppel-like factor 4 (KLF4), while inhibiting CEBPα and GATA2 (Zhu *et al.*, 2016). PU.1 has also been associated with CSF-1R transactivation during differentiation (Zhang *et al.*, 1994).

Table 1.1. Transcription factors known to be associated with monocyte-to-macrophage differentiation

Transcription Factor	Function	References
CEBPα, CEBPβ, CEBPε	Each plays a role in mediating differentiation together with other transcription factors at different stages of differentiation.	(Friedman, 2002)
GATA2	Interacts with PU.1 and regulates differentiation of HSCs into myeloid lineages.	(Walsh *et al.*, 2002; Chou *et al.*, 2009)
IRF8	Promotes monocyte differentiation and inhibits granulocyte production.	(Meraro *et al.*, 1999; Tsujimura *et al.*, 2002; Tamura *et al.*, 2005;)
KLF2	Reduces in expression upon differentiation into macrophages.	(Das *et al.*, 2006, 2012)
KLF4	Expression enhances differentiation and is directly regulated by IRF8.	(Feinberg *et al.*, 2007; Alder *et al.*, 2008; Kurotaki *et al.*, 2013)
SPI1/PU.1	Expression increases during monocyte differentiation. Interacts with other transcription factors to mediate differentiation.	(Nutt *et al.*, 2005; Zhu *et al.*, 2016)

1.7 Promonocytic cell lines as model systems

Cancer-derived human cell lines are important *in vitro* tools for studying cellular activities, processes, responses, and signalling pathways. *In vitro* experiments are preferable, where possible, for the development of specific applications due to the budgetary and/or ethical constraints that are associated with animal and human *in vivo* studies. *In vitro* systems are advantageous due to their natural nature; yet, donor viability and substantial individual diversity complicate the analysis and interpretation of data (Chanput *et al.*, 2014). However, cell lines are malignant in nature and the controlled cultivation of cells like this, in conditions

outside their natural environment, can cause adverse reactions relative to their natural environment (Schildberger *et al.*, 2013).

Promonocytic cell lines are those that have the ability to differentiate into monocytes and therefore, in most cases, macrophages (Tanaka *et al.*, 1983; Koeffler *et al.*, 1984; Kohro *et al.*, 2004; Valdés López and Urcuqui-Inchima, 2018). While they do not entirely reproduce the response spectrum of primary monocyte-derived-macrophages, they can mimic some biological processes and their functional implications (Tedesco *et al.*, 2018). Some of the widely used promonocytic cell lines include the THP-1, U937, HL-60, ML-2 and Mono Mac 6 cell lines. These cell lines differ based on their origins and maturation stages, and their use is context-dependent.

1.7.1 The THP-1 Cell Line

The THP-1 cell line is one of the most widely used promonocytic cell lines in studying monocyte-to-macrophage differentiation (Qin, 2012; Chanput *et al.*, 2014). The THP-1 cell line was isolated by Tsuchiya *et al.* (1980). The cell line was derived from the blood of a one-year old, male patient suffering with acute monocytic leukaemia. In terms of morphology and differentiation, THP-1 cells bear resemblance to primary monocytes and macrophages (Tsuchiya *et al.*, 1980; Auwerx, 1991). However, different levels of gene expression and cytokine release, as well as gene expression at baseline, have been described in some cases (Schildberger *et al.*, 2013; Shiratori *et al.*, 2017).

1.7.1.1 THP-1 cells and their relationship to primary monocytes

Primary monocytes have been shown to produce higher levels of pro-inflammatory cytokines, such as TNFα, IL-6, IL-8 and IL-10, than THP-1 cells (Schildberger *et al.*, 2013) following LPS stimulation. In terms of baseline gene expression levels, primary monocytes were reported to have higher expression levels of genes such as *TNFα, IL-1B, IL-6, CD14* and CD68 relative to undifferentiated THP-1 cells (Bruckmeier *et al.*, 2012). It has been reported that following their differentiation into macrophages, THP-1 cells express genes such as MD2, CD14 and MyD88 - all of which are involved in LPS signalling *in vivo* (Zarember and Godowski, 2002). These cells also mimic primary macrophages in terms of surface marker expression, cell morphology and cytokine production (Kohro *et al.*, 2004; Schroecksnadel *et al.*, 2011; Tedesco

et al., 2018). THP-1 cells are therefore often used as a simplified model of human monocytes and macrophages, rather than an alternative to primary monocytes and macrophages (Tedesco *et al.*, 2018).

1.7.1.2 Differentiation of THP-1 cells

THP-1 cells, when treated with phorbol 12-myristate 13-acetate (PMA) or the active metabolite of vitamin D_3, 1,25 dihydroxyvitamin D_3 (VD_3), can differentiate into a state more phenotypically representative of macrophages (Rovera *et al.*, 1979; Tanaka *et al.*, 1983). While M-CSF is biologically relevant to the differentiation process *in vivo*, it is not frequently used *in vitro* (Chanput *et al.*, 2014). The differentiation of THP-1 cells into this state results in adherence to the culture flask and obvious changes in cell morphology, such as a change in overall cellular shape, nucleus irregularity, and phagocytic vacuoles appearing in the cytoplasm (Auwerx, 1991).

1.7.1.2.1 PMA and Vitamin D_3 as Differentiation-Inducing Agents

PMA is a toxic, tumour-promoting and inflammation-inducing phorbol ester, derived from the unripe fruit of *Sapium indicum*, able to induce differentiation of THP-1 cells into a macrophage-state (Taylor *et al.*, 1981; Chang *et al.*, 2020). On the flipside, VD_3 is naturally occurring and has the ability to induce differentiation into a macrophage-state in THP-1 cells (Munker *et al.*, 1986; Auwerx, 1991). Full differentiation of THP-1 cells into a macrophage-like state occurs at least 48 hours after being incubated with PMA, depending on the concentration applied (Park *et al.*, 2007; Lund *et al.*, 2016). The resting of differentiated THP-1 macrophages without PMA for around 24 h in culture media is essential to increase the expression of macrophage markers and decrease the expression of nuclear factor kappa B (NF-κB) genes up-regulated as a result of the differentiation process. Indicators of successful differentiation are cell adherence, increased phagocytic capacity, and increased expression of surface markers associated with differentiation, including CD14, CD36, TLR2, and complement receptor 3 (CR3) (CD11b/CD18).

Surprisingly, given the toxic nature of PMA, descriptions of the cytotoxic effect of the agent on THP-1 cells in the literature are few and far between (Browne *et al.*, 2022; Lund *et al.*, 2016; Park *et al.*, 2007). These studies have reported an average cell viability of ~92.55% when treated with PMA for 72 hours (Browne *et al.*, 2022) and 93% when treated with concentrations

ranging from 5 ng/ml - 125 ng/ml for 48 hours (Lund *et al.*, 2016). With respect to the effect of VD_3 on the viability of THP-1 cells, a study performed by Wu *et al.*, (2022) demonstrated that viability decreases significantly in a concentration- and time-dependent manner, but to a lesser extent than after PMA treatment (Wu *et al.*, 2022). Despite the increased viability, treatment with VD_3 results in a less mature macrophage phenotype relative to PMA (Schwende *et al.*, 1996; Valdés López and Urcuqui-Inchima, 2018). With respect to production of interleukin-1 beta (IL-1B) and TNFα and phagocytic activity, the macrophages resulting from treatment with 100 nM VD_3 for three days were found to be less similar to primary monocyte-derived macrophages than THP-1 macrophages produced using 200 nM PMA for three days (Auwerx, 1991; Daigneault *et al.*, 2010). Furthermore, it has been shown that VD_3 treatment, while associated with an increase in monocytic markers, displays little to no changes in cell morphology relative to that of PMA treatment (Valdés López and Urcuqui-Inchima, 2018). Evidently, the full effect of either treatment on THP-1 cells is not clear.

1.8 Vitamin D_3 as an Immunomodulator

VD_3 generally occurs in its biologically inert form (Holick, 2009), however, hydroxylation at carbon 25 of its side chain into 25-hydroxyvitamin D_3 (25(OH)D), occuring in the liver (Lips, 2006), and additional hydroxylation at carbon 1 within its A-ring, produces the active metabolite, $1,25(OH)_2D_3$ (Figure 1.4; Lips, 2006). $1,25(OH)_2D_3$ is a lipophilic molecule, as such, it readily traverses biological membranes and binds to the nucleus-based transcription factor, vitamin D receptor (VDR; (DeLuca, 2014)) with high affinity (kD = 0.1 nM).

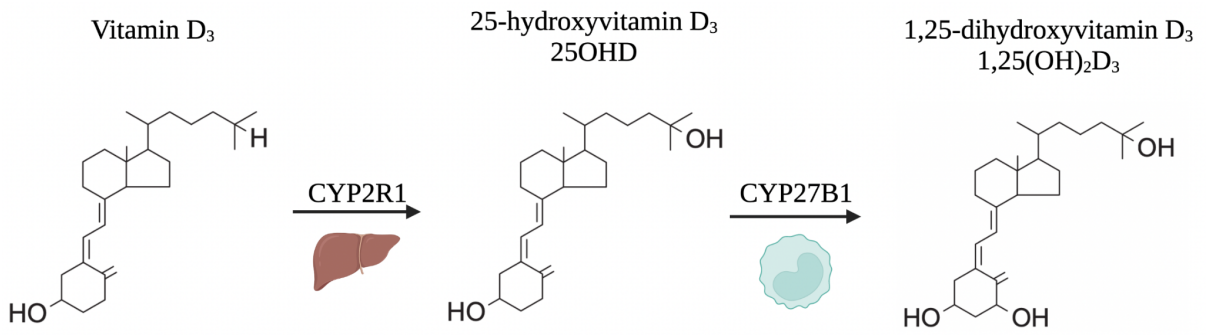

Figure 1.4: The hydroxylation of vitamin D_3 to its active metabolite 1,25-dihydroxyvitamin D_3 ($1,25(OH)_2D_3$). Vitamin D_3 is derived from the diet or UV rays and undergoes metabolism in the liver, where the compound is hydroxylated at carbon 25 of its side chain into 25-hydroxyvitamin D_3 (25(OH)D). In an intracrine manner, further hydroxylation at carbon 1 within its A-ring occurs in cells such as monocytes and/or macrophages. This also occurs in the kidneys via CYP27A1. This second hydroxylation step results in the production of the biologically active form of the metabolite, $1,25(OH)_2D_3$. (Image created in www.biorender.com)

During haematopoiesis, VDR functions with the transcription factors, PU.1 and CEBPα, as a critical regulator of myeloid differentiation in immune cells such as monocytes and granulocytes (Novershtern *et al.*, 2011). Furthermore, VDR is activated through the TLR1/2 pathway, where cytochrome P450 Family 27 subfamily B member 1 (CYP27B1) is a target of VDR (Liu *et al.*, 2006). Monocytes, macrophages and dendritic cells express the mitochondrial VD_3 activating enzyme, CYP27B1, and therefore through the TLR1/2 pathway the localised conversion of 25(OH)D to $1,25(OH)_2D_3$ is induced in these cells (Liu *et al.*, 2006). $1,25(OH)_2D_3$ binds to VDR and the retinoid X receptor (RXR) in the cytoplasm and this complex is translocated to the nucleus where it binds to vitamin D response elements (VDRE) located in regulatory regions of VD_3 target genes, inducing the transcription of VD_3-responsive genes and leading to increased production of antimicrobial proteins such as cathelicidin and β-defensin (Figure 1.5; Liu *et al.*, 2006; Medrano *et al.*, 2018). It is thus clear that VD_3 plays an essential role as an immune modulator in monocytes and macrophages. Despite this, however, the exact mechanisms and impact VD_3 has on monocyte-to-macrophage differentiation remains unclear. One way in which questions related to VD_3-mediated differentiation can be addressed

is through omics studies in which differentiated end-states induced by VD_3 are compared to those induced by PMA.

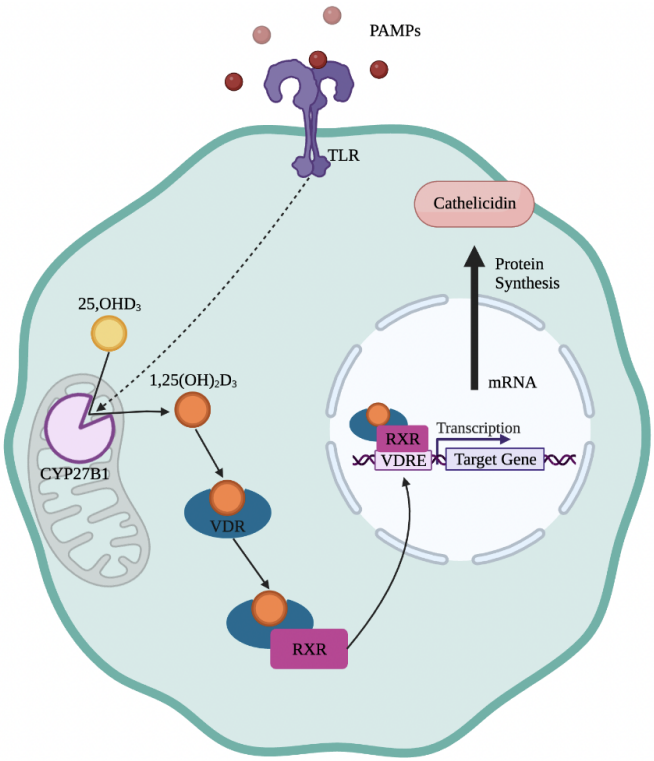

Figure 1.5: TLR/VD_3-mediated production of antimicrobial peptides in monocytes/macrophages. Upon interaction of TLR1/2, CYP27B1 is activated and circulating 25-hydroxyvitamin D_3 (25(OH)D) is metabolised into 1,25 dihydroxyvitamin D_3 ($1,25(OH)_2D_3$). $1,25(OH)_2D_3$ binds to the vitamin D receptor (VDR) and the retinoid X receptor (RXR) in the cytoplasm. The $1,25(OH)_2D_3$/VDR/RXR complex translocates into the nucleus, where it binds to the vitamin D response element (VDRE) located in the regulatory region of a VD_3 target gene. Transcription of the target gene is induced and antimicrobial peptides such as cathelicidin are produced (Image created in www.biorender.com; Liu *et al.*, 2006; Medrano *et al.*, 2018)

1.9 RNA-sequencing and Differential Gene Expression

RNA-sequencing (RNA-seq) has become a popular tool in molecular biology, especially as a tool for differential gene expression (DGE) analysis (Stark *et al.*, 2019; Zhang *et al.*, 2014). This approach provides the means to quantify changes in gene expression levels across different conditions at genome-wide scale. RNA-seq makes use of deep sequencing and next generation sequencing (NGS) technologies (Stark *et al.*, 2019). The RNA-seq approach involves the extraction of RNA, mRNA enrichment or ribosomal RNA depletion, fragmentation, cDNA synthesis, and the production of an adaptor-ligated sequencing library. These adapter-ligated sequences are then sequenced using a high throughput sequencing platform. The generated sequencing reads are then mapped to a reference genome or transcriptome. Gene expression levels can then be estimated and compared across two or more conditions. This enables changes in expression levels across conditions to be statistically evaluated (Oshlack *et al.*, 2010). A host of tools have been developed that allow the identification of these differentially expressed genes.

1.10 Problem statement

Monocyte and macrophage heterogeneity and differentiation is not yet completely understood. In an attempt to address this, promonocytic cell lines are used as model systems. While both PMA and $1,25(OH)_2D_3$ induce monocyte-to-macrophage differentiation, and despite the host of studies that have utilised this model system to study monocyte/macrophage function and differentiation (Kramer and Wray, 2002; Hjort *et al.*, 2003; Liu *et al.*, 2022; Wu *et al.*, 2022), differences in their mechanisms of action, as well as how the end states of the differentiation process differ, are not well understood. Studies have, and continue to try to address this (Schwende *et al.*, 1996; Kohro *et al.*, 2004; Lund *et al.*, 2016; Valdés López and Urcuqui-Inchima, 2018), however no reference exists for a definite choice and/or preference for either agent based on its nature (i.e., toxic or naturally-occurring) and its impact on the cell. In addition, the heterogeneity associated with monocytes and macrophages and their differentiation poses further limitations on this. Where other studies encompass a targeted approach to this issue, where differentiation is studied with additional stimulants, this study addresses this issue by studying the entire gene expression profile of these cells following stimulation with only the differentiation agents.

1.11. Aim and Objectives

Therefore, the aim of this study was to use computational approaches to compare the effects of PMA and $1,25(OH)_2D_3$ on the differentiation of monocytes into macrophages, using the promonocytic THP-1 cell line.

The study aim was achieved through the following objectives:

1. To perform transcript quantification on RNA-seq data obtained from untreated, PMA-treated and $1,25(OH)_2D_3$-treated THP-1 cells, using pseudoalignment.
2. To perform differential gene expression analysis between untreated and PMA-treated THP-1 RNA-seq data and between untreated and $1,25(OH)_2D_3$-treated THP-1 cells.
3. To identify and characterise genes uniquely differentially expressed in THP-1 cells in response to treatment with PMA.
4. To identify and characterise genes uniquely differentially expressed in THP-1 cells, in response to treatment with $1,25(OH)_2D_3$.
5. To identify and characterise genes differentially expressed in THP-1 cells in response to treatment with both PMA and $1,25(OH)_2D_3$.

Chapter 2: Methodology

2.1 Data Acquisition

Publicly available RNA-seq data was obtained from the European Nucleotide Archive (ENA) (www.ebi.ac.uk/ena/). RNA-seq data derived from untreated promonocytic THP-1 cells, as well as cells treated with either 100 ng/ml PMA or 500 nM $1,25(OH)_2D_3$ (VD_3) for 72 hours was acquired (Accession number: PRJNA449980; Liu *et al.*, 2018). The concentrations of PMA used to differentiate THP-1 cells are variable and range from 10 to 400 ng/ml. Furthermore, the period of differentiation ranges from 1-5 days (Chanput *et al,* 2014; Starr *et al*, 2018). Therefore, Liu and colleagues leveraged a common PMA concentration and differentiation protocol. The concentration of VD_3 used, however, is not a common or widely used concentration. Experimental procedures performed by Liu and colleagues to produce this data (Figure 2.1) included total RNA extraction using the RNeasy Mini Kit and QIAshredder (Qiagen), all biological assays were performed in triplicate. DNase treatment was performed and only RNA with an integrity number (RIN) > 8 was used for library preparation. RNA sequencing libraries were prepared using the TruSeq Stranded mRNA Library Prep Kit (Illumina). Paired-end sequencing was performed using the HiSeq 2500 System (Illumina), which resulted in reads of length 100 base pairs (bp). Read 1 was derived from the antisense strand and read 2 from the sense strand. Each condition was sequenced in triplicate.

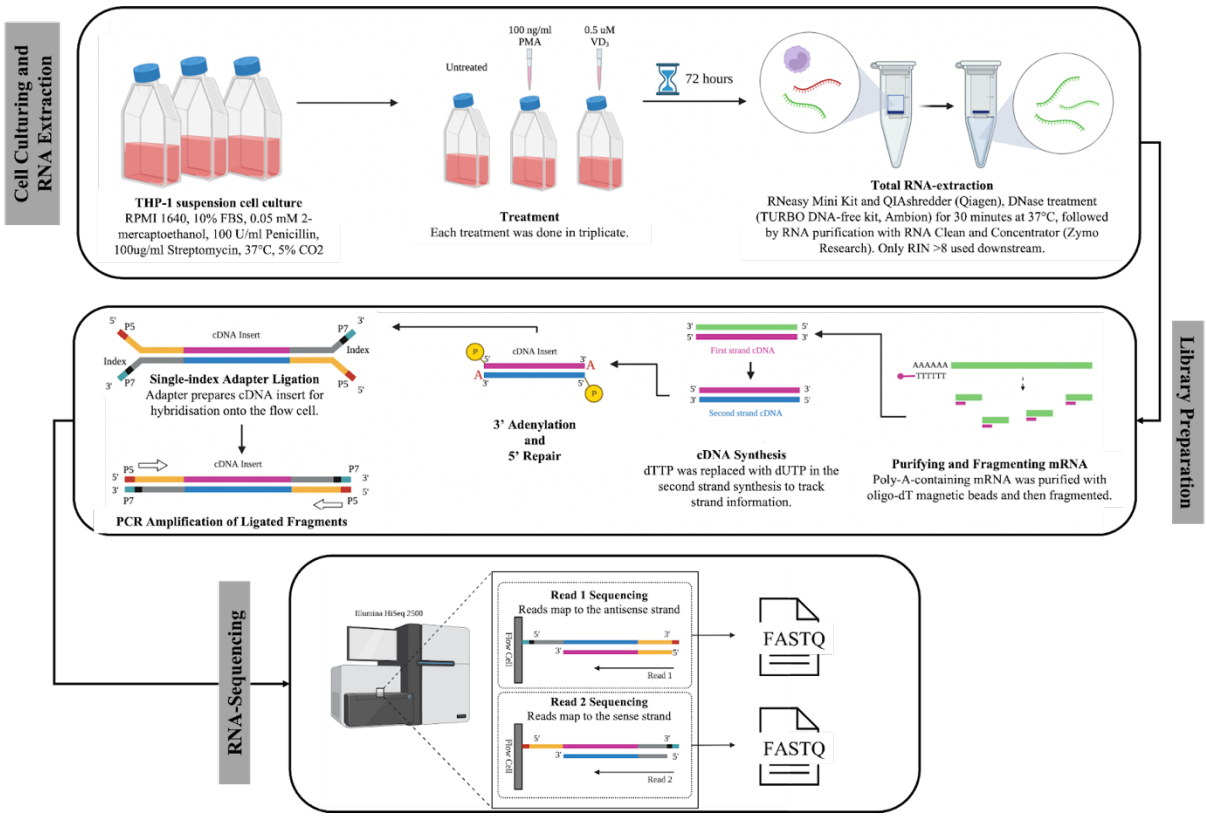

Figure 2.1: Experimental procedure carried out by Liu *et al.* (2018) to produce the RNA-seq data used in this study. THP-1 cells were cultured in suspension and treated with PMA or 1,25$(OH)_2D_3$ (VD_3). Total RNA was extracted and purified. Library preparation for RNA-seq was performed using the TruSeq Stranded mRNA Library Prep Kit (Illumina). This consisted of polyA-containing mRNA extraction, cDNA synthesis, 3' adenylation and 5' repair, adapter ligation and PCR amplification. Sequencing was performed using the HiSeq 2500 System (Illumina), which resulted in fastq files with paired-end reads with a length of 101 base pairs.

2.2 RNA Sequencing Data Quality Control

Quality control of sequencing data was performed using FastQC (www.bioinformatics.babraham.ac.uk/projects/FastQC/). FastQC assesses sequence data quality based on predetermined metrics and classifies each metric as a 'pass', 'warning' or 'fail'. These metrics take into consideration factors that affect sequencing quality, such as the quality of each base sequenced, as well as additional attributes such as average sequencing depth with respect to the distribution of sequencing reads per sequencing file.

By performing this quality control step, the aim was to identify poor, bad quality sequences that may influence downstream applications. According to the FastQC metrics, poor quality sequences can be defined as sequences having a per base quality < 20 at various positions in the read. In addition, when a large proportion of sequences have an overall quality score < 27 and a valid base was not called in >20% of the sequence, the sequence was considered to be of poor quality ("Babraham Bioinformatics - FastQC A Quality Control tool for High Throughput Sequence Data," n.d.). Additional metrics that were assessed include the number of reads, to identify the average sequence depth of the samples, as well as duplication levels. With respect to duplication levels, FastQC tends to flag this metric in the case of RNA-seq data as the differences in expression of transcripts are read as 'duplicated' sequences.

2.3 Transcript Quantification

Pseudoalignment is an approach that enables sequencing reads to be mapped to an indexed reference transcriptome, allowing transcript abundance to be quantified. Pseudoalignment has been shown to be faster and more accurate than traditional alignment methods (Sarantopoulou et al., 2021). This approach is capable of processing 30 million paired-end RNA-seq reads in less than 10 minutes (Bray *et al.*, 2016). Furthermore, tools utilising pseudoalignment have been shown to have up to 85% accuracy and are comparable with that of traditional aligners (Bray *et al.*, 2016; Sarantopoulou *et al.*, 2021).

Among the common tools that adopt this pseudoalignment approach are kallisto (Bray *et al.*, 2016) and Salmon (Patro *et al.*, 2017). The latter incorporates an efficient 'quasi-mapping' method (Srivastava *et al.*, 2016). In addition to this, RNA-seq specific biases such as positional biases in coverage, sequence-specific biases at the 5′ and 3′ ends of sequenced fragments, fragment-level GC content bias, strand-specific procedures, and the fragment length distribution are all taken into account with Salmon when computing transcript abundances. Accounting for these biases increases the correlation between expression estimates derived from sequence data generated using different sample preparation methods and different sequencing technologies (Roberts *et al.*, 2011).

2.3.1 Indexing the Reference Transcriptome

Transcript abundance was quantified against a decoy-aware, indexed reference transcriptome based on the most recent version of the human reference genome, GRCh38.p13, and the Gencode v40 transcript annotations (Frankish et al., 2019). This was obtained using the `salmon index` command. Indexing breaks down the reference genome into indices that enable the Salmon to efficiently narrow down the potential genomic origins of a query sequence.

Decoy-aware mapping is recommended because there may be reads that originate from regions of the transcriptome that are unannotated, but are similar in sequence to annotated regions of the transcriptome. These are known as decoy sequences and including a decoy-aware transcriptome reduces spurious/false positive mapping of these reads to the transcriptome and therefore improves quantification (Sarkar et al., 2017).

2.3.2 Quasi-mapping to determine the origin of sequencing reads

Quasi-mapping uses a k-mer-based approach where the read is searched in k-mers (with a default length of 31bp) against a reference transcript. When a match is found between the k-mer and the reference transcript, the match is extended for the longest possible length. This continues for the length of the read. To obtain final mappings, all matches between k-mers for the read and the reference transcriptome are obtained, together with their location and orientation, and are returned as quasi-mappings of the read. Through quasi-mapping, only the potential origin of the reads are determined, without a base-by-base alignment. This enables faster transcript quantification (Srivastava *et al.*, 2016).

The quasi-mapping procedure was implemented by means of the following command line statement:

```
salmon quant -i /path/to/indexed/transcriptome -l A \
     -1 /path/to/read1 \
     -2 /path/to/read2 \
     -p 8 \
     --recoverOrphans \
     -o
     --seqBias \
```

```
--gcBias \
--validateMappings
```

The `-l A` flag was used for automatic detection of the library type of the reads. The library type of the reads consists of three pieces of information: relative orientation of the reads, strandedness and directionality of the reads. The relative orientation of the reads (Figure 2.2) is applicable in the case of paired-end sequencing, as is the case with this study, where the orientation of the reads is classified as inward-facing, outward-facing or matching. The strandedness of the library refers to whether the reads are stranded or unstranded. In a stranded library, such as the one utilised in this study, reads sequenced from the sense and antisense strands are able to be differentiated and mapped to the appropriate strand, whereas in an unstranded library, reads sequenced from the sense and antisense strands are not differentiated (Levin *et al.*, 2010). Lastly, directionality of the reads is only relevant in the case of stranded libraries where the strand from which the read is derived is determined. Correct identification of the library type is important for more accurate quantification.

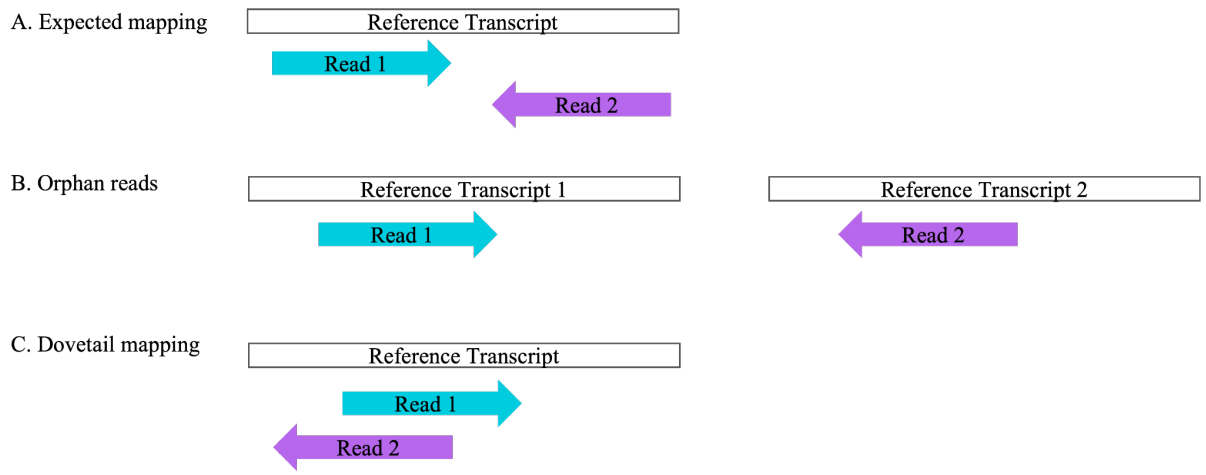

Figure 2.2: Orphan read recovery and dovetail mappings. A) Paired end read mapping to a reference transcript as expected, based on the sequencing library configuration. B) Orphan reads occur when one of the reads from the pair maps either further upstream or downstream than expected based on the sequencing library configuration. C) Dovetail mapping occurs when the first mapped base of the reverse read (Read 2) is upstream of the first mapped base of the forward read (Read 1), creating a 'dovetail' effect.

In the event where only one of the paired reads map to a region of the reference that is not expected based on the library configuration, the `--recoverOrphans` flag enables the missing read to be recovered by searching upstream and downstream of the mapping position to place the read appropriately (Figure 2.1B). In terms of dovetail mappings, where the first mapped base of the reverse read is upstream of the first mapped base of the forward read (Figure 2.1C), the default was maintained and these mappings were excluded.

Lastly, the `--validateMappings` flag was invoked to enable what is termed selective alignment. Selective alignment enables the mappings to be scored and validated. Exact matches between the read and transcriptome are obtained, and the relevant transcripts are then extracted. The matches are scored, and potential putative mapping sites for a read are identified. For paired end reads, the read pair is matched, allowing the mapping loci for the entire fragment to be determined. The potential mapping loci are then assigned scores and considered relative to the decoy sequences for validity (Srivastava *et al.*, 2020). Selective alignment is an approach that addresses both the specificity and sensitivity problems of lightweight mapping. It involves increased mapping sensitivity along with a more exhaustive scoring approach for possible mappings that also allows specific details of the quality of the mapping to be obtained. Furthermore, selective alignment produces mappings results more consistent with that of traditional alignments (Srivastava *et al.*, 2020).

2.3.3 Estimation of transcript and gene abundances

Following quasi-mapping, final transcript abundance estimates were computed through the `Salmon quant` command. Salmon does not simply count the reads mapping to the reference transcripts but rather, statistically computes these estimates by applying sample-specific bias models that account for known biases in RNA-seq data. RNA-seq data can be subject to such sample-specific biases as a result of RNA extraction and library preparation procedures (Love *et al.*, 2016). Some of the biases that are considered are fragment-length distribution, which is introduced during size selection of library preparation, and strand-specific bias.

A number of factors influence the likelihood of a fragment being selected for sequencing and one of these factors is the sequences surrounding the 3' and 5' ends of the fragment. These biases are introduced during the priming stage of RNA extraction where oligio-d(T)

nucleotides shift the base content at the beginning of the fragment or random hexamers have differential binding efficiencies (Li *et al*., 2010; Roberts *et al*., 2011; Love *et al*., 2016). Salmon applies two variable length Markov models (VLMM) to account for this bias. These models were applied through the `--seqBias` flag in the command line statement.

Another known bias that needs to be accounted for in RNA-seq is GC-content - where the number of G and C nucleotides in the fragment impacts its likelihood of being sequenced (Risso *et al.*, 2011). This bias can be introduced at various stages of the sequencing processes, such as PCR amplification, cluster amplification and sequencing itself (Aird *et al.*, 2011). Both GC-rich and GC-poor regions have been shown to be under-represented in RNA-seq, which tends to favour coverage of regions where the GC-content is balanced. Salmon accounts for this bias through two models, one that models the distribution of reads for all possible GC-content values and another that models this distribution for the known reference transcripts (Patro *et al.*, 2017). These models were applied through the `--gcBias` flag in the command line statement.

Salmon considers all these factors together with the quasi-mappings to estimate final transcript abundances. This resulted in a quantification file (quant.sf) for each sample, as well as a number of auxiliary files. Data in the quantification file is organised into a n x m matrix, where the five columns represent the name of the transcript, the length of the transcript, the effective length of the transcript (accounting for the sequence-specific and GC bias), the transcripts per million (TPM) value and the number of reads mapping to each transcript that was quantified (i.e. the transcript abundance).

2.4 Differential Gene Expression Analysis

In order to import quantification files produced with Salmon into the R environment, the R/Bioconductor tool, tximeta (Love *et al.*, 2019) was used. The tool leverages its primary package, tximport (Soneson *et al.*, 2016), and aggregates transcripts-level counts to the gene-level. Gene-level estimates are more accurate when derived from aggregated transcript-level counts, as opposed to when they are derived from gene-based count methods like HTSeq (Soneson *et al.*, 2016). Thus the need for transcript-to-gene-level aggregation.

A metadata table for the samples used in this study was constructed, which included the sample identifiers, their associated condition (untreated, PMA-treated and VD_3-treated), and the file path to the corresponding Salmon quantification file. Tximeta summarises this metadata and the count data into an object known as a SummarisedExperiment (Figure 2.3). The SummarisedExperiment was then passed through the `summariseToGene` function to obtain a gene-level summarised experiment (Love *et al.*, 2019). SummarizedExperiment objects store multiple matrices of data, referred to as 'assays'. These matrices include the Salmon outputs, raw read counts, effective transcript lengths, and TPM abundances. The rows in the SummarisedExperiment object represent genomic features (transcript/gene identifiers) and are linked to transcript annotations derived from the reference transcriptome (Figure 2.3). Any sample metadata provided is also attached to the SummarizedExperiment. The implementation of tximeta allowed Salmon quantification files to be imported into the R/Bioconductor environment and the count data to be aggregated to the gene-level in preparation for differential gene expression analysis.

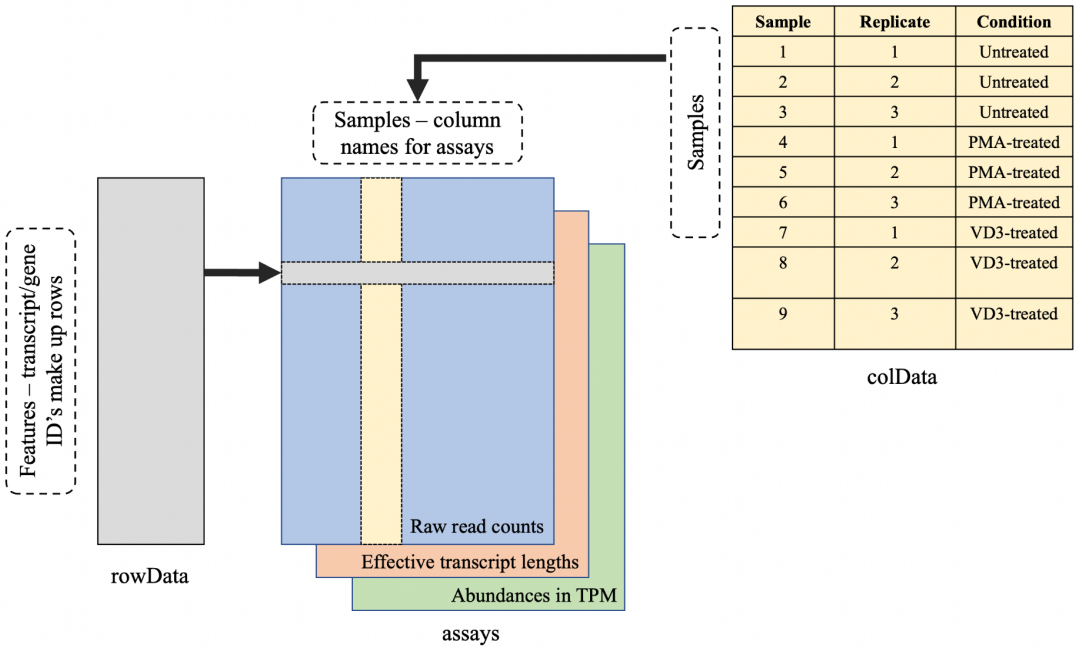

Sample	Replicate	Condition
1	1	Untreated
2	2	Untreated
3	3	Untreated
4	1	PMA-treated
5	2	PMA-treated
6	3	PMA-treated
7	1	VD3-treated
8	2	VD3-treated
9	3	VD3-treated

Figure 2.3: SummarisedExperiment object layout. Sample information such as condition and sample identifier is stored in colData, and makes up the column names of the assays. The SummarisedExperiment object consists of three assays derived from Salmon: raw, unnormalised read counts, effective transcript lengths, and transcript abundances normalised as TPM. The features are stored in rowData and make up the rows of the assays. In the case of a SummarisedExperiment these features are transcript identifiers, and in the case of a gene-level SummarisedExperiment , they are gene identifiers.

Differential gene expression analysis was performed by comparing both the PMA-treated and the VD_3-treated THP-1 data against the untreated control data, in order to identify the changes in gene expression associated with each treatment. From the genes that were quantified, all genes with a mean count of zero, across all samples, were removed, as well as all genes with a mean count less than 10, across all samples. This resulted in a total of 17 504 genes to be assessed for differential gene expression. The R/Bioconductor package, DESeq2 v1.30.1 (Love *et al.*, 2014) was employed to do this. DESeq2 was utilised in this study because it incorporates an automatic independent filtering step, as well as automatic outlier detection and handling. DESeq2 also incorporates a 'shrinkage' function, which enhances reliability and reproducibility, and is suitable for small sample testing (Love *et al.*, 2014).

The `DESeq` function included in the DESeq2 package 'wraps' three key functions into a single function. First it carries out the `estimateSizeFactors` function, which allows the mean of the read counts for each gene to be normalised for differences in sequencing depth and library composition. Sequencing depth refers to the number of times a particular nucleotide is sequenced in a given sequencing experiment. Given that read lengths are short and sequencing errors may occur, higher coverage allows for greater confidence in the bases called (Sims *et al.*, 2014). Normalisation on the basis of differences in sequencing depth is important during differential expression studies so as to not to mistake these differences for differences in expression. Library composition refers to the composition of the RNA itself. Factors that are considered include differences in the number of genes expressed between samples or only a few highly differentially expressed genes between samples. These factors need to be accounted for to more accurately determine differentially expressed genes. DESeq2 accounts for these biases by scaling the mean by a size factor using a log-based approach. Here, the geometric mean for each gene across all samples is calculated and every original gene count is then divided by its corresponding geometric mean. The size factor of each sample is the median of these ratios.

This is followed by dispersion estimation through `estimateDispersions`. Dispersion is defined as the gene-wise variability between the biological replicates of each treatment condition. DESeq2 determines these estimates and normalises them through an approach termed 'shrinkage', which is performed in three main steps. Firstly, the gene-wise estimates (i.e. estimates based on the mean expression level of the genes between replicates) of dispersion are computed through a maximum likelihood approach (i.e. given the expression levels, the most likely dispersion is estimated). When working with a small number of replicates (three to six) per sample, genes with similar means tend to show large differences in dispersion. This makes the gene-wise dispersion estimates unreliable. DESeq2 (Love *et al.*, 2014) addresses this issue by sharing information across genes, and assuming that genes with similar mean expression levels will exhibit similar dispersion. Secondly, a curve is fitted to the gene-wise dispersion estimates. This curve provided a consensus of accurate estimates of the dispersion expected for certain levels of expression. Lastly, the gene-wise estimates computed initially are involved in a 'shrinkage' step where they are shrunk towards the fitted curve. These newly computed estimates are then more indicative of accurate dispersion given the mean expression level. It should be noted that dispersion can be underestimated, making that particular gene

more likely to be called incorrectly as differentially expressed in a comparison. In this situation, shrinkage results in a raised dispersion estimate, reducing type I error (false positives). In cases of extreme outliers (estimates within more than two standard deviations above the fitted curve), where shrinkage results in greatly reduced estimates, the gene-wise estimates are used, to reduce type I error calls (Love *et al.*, 2014).

Lastly, the `nbiomWaldTest` function is performed. DESeq2 models the read counts along a negative binomial distribution. This distribution is used because it is able to capture the overdispersion that biological replicates introduce. The negative binomial distribution allows for the variance to exceed the mean, which is not the case in a Poisson distribution, for example, where the variance is expected to be equal to the mean. In modelling the counts with a negative binomial distribution, the mean and the dispersion needs to be estimated, the accuracy of which increases with the number of replicates. However, since most RNA-seq experiments only make use of 2-3 replicates, as is the case in this study, DESeq2 compensates for this by dispersion estimation and subsequent 'shrinkage' of the dispersion estimates, as aforementioned.

The function further fits a general linear model (GLM) to the counts of each particular gene within a sample. This results in a coefficient of the overall expression levels of the gene, as well as an estimation of the $\log_2$ fold change in expression between the untreated and treated samples to be returned. The $\log_2$ fold changes, together with a standard error for each of these estimates, are then used in the hypothesis testing (Love *et al.*, 2014). The null hypothesis assumes that there is no significant difference between the average read count values of the different treatment conditions for any particular gene. A z-statistic is obtained by dividing the shrunken $\log_2$ fold change estimate by its standard error and comparing it to a standard normal distribution. Following an automatic independent filtering step, the p-values obtained from the Wald test were corrected for multiple testing using the Benjamini Hochberg procedure (Benjamini and Hochberg, 1995).

When running a single hypothesis test, the possibility of a gene being incorrectly called as differentially expressed, i.e. a false positive, is considered to be relatively small. However, when a large number of hypothesis tests/comparisons are being performed, as is the case when testing for differential gene expression, a multiple testing problem is introduced, where the number of possible false positive calls can potentially increase dramatically. Controlling the

false discovery rate (FDR) by introducing an adjusted p-value is a useful way to correct for this multiple testing problem. This is also associated with a loss of power because the FDR for a set of genes will likely be higher than the p-values of these genes. To circumvent this, DESeq2 determines a filtering threshold by maximising the number of genes found at a user-defined target FDR, thereby omitting the genes that have little or no chance of being called as differentially expressed from multiple testing adjustments. An adjusted p-value threshold of < 0.05 was used to identify significantly differentially expressed genes in both treatment conditions (PMA-treated relative to untreated and VD_3-treated relative to untreated cells) together with a log2(fold change) threshold of 1. This meant that only genes with an absolute fold change of 2 and above were considered.

2.6 Over-representation/Enrichment Analysis

The gene lists resulting from the differential gene expression analysis alone are unable to describe the intricate biological mechanisms at play in any given treatment condition. An over-representation analysis (ORA)/enrichment analysis allows the evaluation of the proportion of query genes (in this case, differentially expressed genes) that belong to a group of tested genes. These "groups of tested genes" refer to information found in the Gene Ontology (GO; Ashburner *et al.*, 2000) and the Kyoto Encyclopaedia of Genes and Genomes (KEGG; Kanehisa *et al.*, 2010) databases. These databases outline biological pathways and processes and their associated genes. In an ORA, the statistical significance of the overlap between the query genes and the pathway genes is often calculated using a hypergeometric test. A set of background genes, known as the 'universe', is required for this. The 'universe' refers to all the genes in the profiled dataset that were considered, i.e., all the genes that were sequenced and quantified. The basis of this type of analysis is that pathways that strongly overlap with the query genes are associated with biological phenomena involving these genes (Wieder *et al.*, 2021). The output from such an analysis consists of a list of genes that are enriched within certain processes and pathways and their associated statistical significance (p-value).

While the basic infrastructure of available enrichment tools tends to be the same, they differ in terms of the gene set database used, the overall interface and the data visualisation techniques employed (Huang *et al.*, 2009; Karp *et al.*, 2021). Each tool however requires an annotation database, followed by algorithms and statistical methods to determine enrichment and an

associated p-value, and lastly, each tool requires a method for presentation of the results (Huang *et al.*, 2009). Algorithms to quantify enrichment scores generally incorporate two ratios: the number of significantly expressed genes in a pathway (from the differentially expressed gene list) relative to the number of all the genes in that pathway (from the pathway database), and the number of significantly expressed genes relative to all genes in any pathway (Karp *et al.*, 2021). Various statistical methods such as a Fisher's exact test, chi-square test, hypergeometric distribution and binomial distribution are then used to obtain a p-value (Huang *et al.*, 2009). clusterProfiler (Wu *et al.*, 2021; Yu *et al.*, 2012) is an R/Bioconductor package that allows for the determination and visualisation of enriched genes. This tool was utilised in this study as it provides a wide range of visualisation options for the enrichment results.

The over-representation analysis facet of clusterProfiler utilises various pathways databases such as GO, KEGG, wikiPathways, Reactome, Disease Ontology and Medical Subject Headings (MeSH). The GO and KEGG databases were utilised in this study as they are well established, with rigorous curation. These are manually curated databases that obtain their information from the scientific literature (Ashburner *et al.*, 2000; Kanehisa *et al.*, 2010). They provide repositories that allow clusterProfiler to access various pathway annotations. A limitation of overrepresentation analysis is that genes within a particular GO term are treated with equal importance, and therefore a change in expression of a gene that may regulate genes within the pathway will have a greater effect than the change in expression of one of the target genes.

The DEG list was input into the `enrichGO` function for GO enrichment. The universe was provided as a list of all the genes quantified for each corresponding treatment. Gene function annotations are classified according to three aspects in the GO consortium. These are: molecular function, cellular component and biological process, which pertains to the molecular activities of the gene product, the location where the gene product functions and the process in which the gene product functions, respectively (Ashburner *et al.*, 2000; Balakrishnan *et al.*, 2013). Accordingly, the ontology was specified as molecular function ('`MF`'), cellular component ('`CC`') or biological process ('`BP`') within the function.

A hypergeometric distribution, which is a discrete probability distribution, was used, thereby representing the probability of observing the number of experimentally differentially expressed

genes in the pathway of interest and the total number of genes in that annotated pathway according to the provided universe, without replacement, relative to the total number of pathway-related genes in the database (Karp *et al.*, 2021; Yu *et al.*, 2012). Through this, p-values for each GO term were obtained, which were then subject to correction for multiple testing (Yu *et al.*, 2012). The multiple testing adjustment method was set to the Bejamini Hochberg procedure with "`BH`", and the significance threshold was set to $\alpha = 0.05$. This produced a matrix of GO terms and their corresponding IDs, gene counts indicating the number of genes enriched for that term, corresponding lists of these genes, and their associated p-values and adjusted p-values.

The `enrichKEGG` function was also used, as it allows a KEGG enrichment analysis to be performed. Here, the organism was specified as *Homo sapien* and the relevant gene list was used as input. The p-value threshold was set to $\alpha = 0.05$. Like GO enrichment, `enrichKEGG` utilises a hypergeometric distribution. This produced a matrix of KEGG IDs, as well as associated descriptions of the relevant pathways, together with their associated p-values and adjusted p-values. The tool, pathview (Luo and Brouwer, 2013), was utilised (through the `pathview` function) to produce visualisations of the corresponding KEGG pathway maps, colour-coded by level of gene expression.

2.7 Data and Code Availability

The data used to generate the findings in this study was generated by Liu *et al.*, (2018) and is publicly available in the ENA under the accession number PRJNA449980. All code used to generate the findings in this study can be found at https://github.com/keldacp/masters.

Chapter 3: Results

3.1 Quality Control of RNA Sequencing Data

Quality control analysis of the RNA sequencing data used in the study revealed the raw, unnormalized data to be of high quality. The per base sequence quality was found to be both high (Phred quality scores > 30) and comparable across replicates and treatment conditions (Figure 3.1A). The average sequencing depth was also found to be reasonably similar across replicates and treatment conditions, with untreated samples, PMA-treated samples, and VD_3-treated samples having an average of 50 247 522, 49 845 403, and 62 968 490 sequencing reads per sample, respectively (Figure 3.1B).

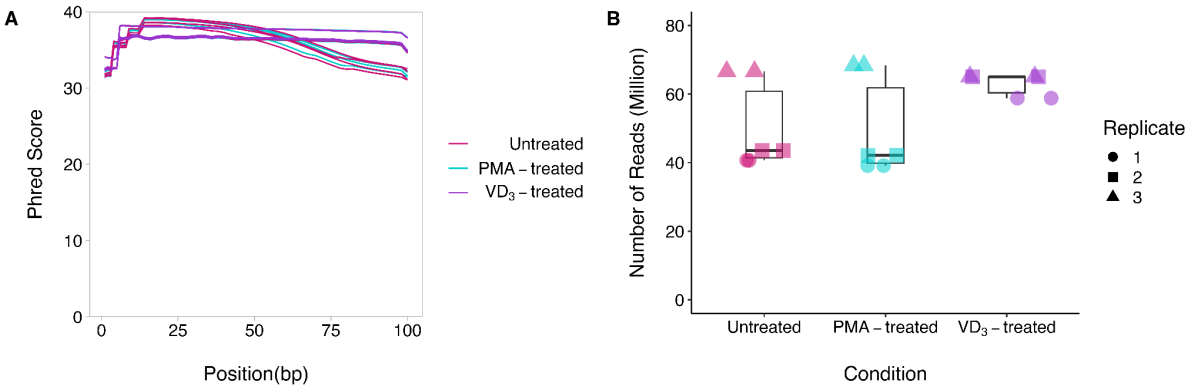

Figure 3.1: General Quality Control Statistics of Raw, Unnormalised Data. A) Per base sequence quality for all sequencing files per sample show all samples with a Phred quality score > 30. B) Distribution of sequencing reads per sequencing file (two per replicate as a result of paired-end sequencing).

3.2 Quality Control of Mapping Data

A total of 389 236 755 sequencing reads were quasi-mapped to 178 398 reference transcripts across all nine sequencing samples included in this study. All samples had a mapping rate of > 85% (Figure 3.2), meaning virtually all the sequencing reads in each sample were successfully assigned to a position within the reference transcriptome and used to estimate transcript abundances. These values take into account the reads that were recovered during orphan rescue, those not mapped as a consequence of failing to reach the alignment score threshold, and discarded dovetail mappings (Figure 3.3).

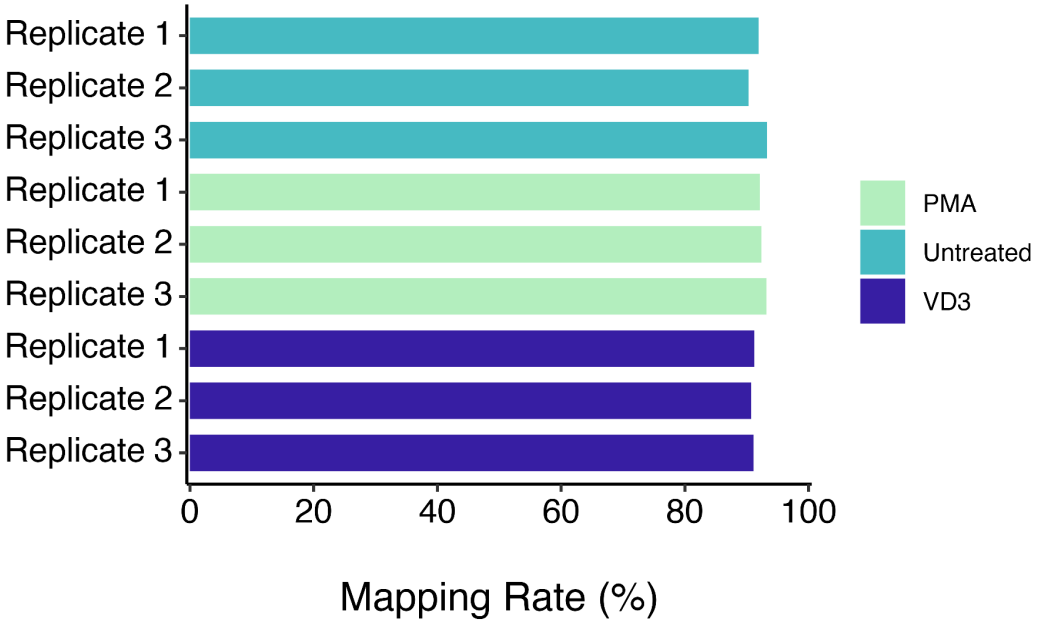

Figure 3.2: Sample mapping rates. The percentage of reads quasi-mapped to the reference transcriptome (GRCh38.p13, and the Gencode v40 transcript annotations) was > 85% for all samples.

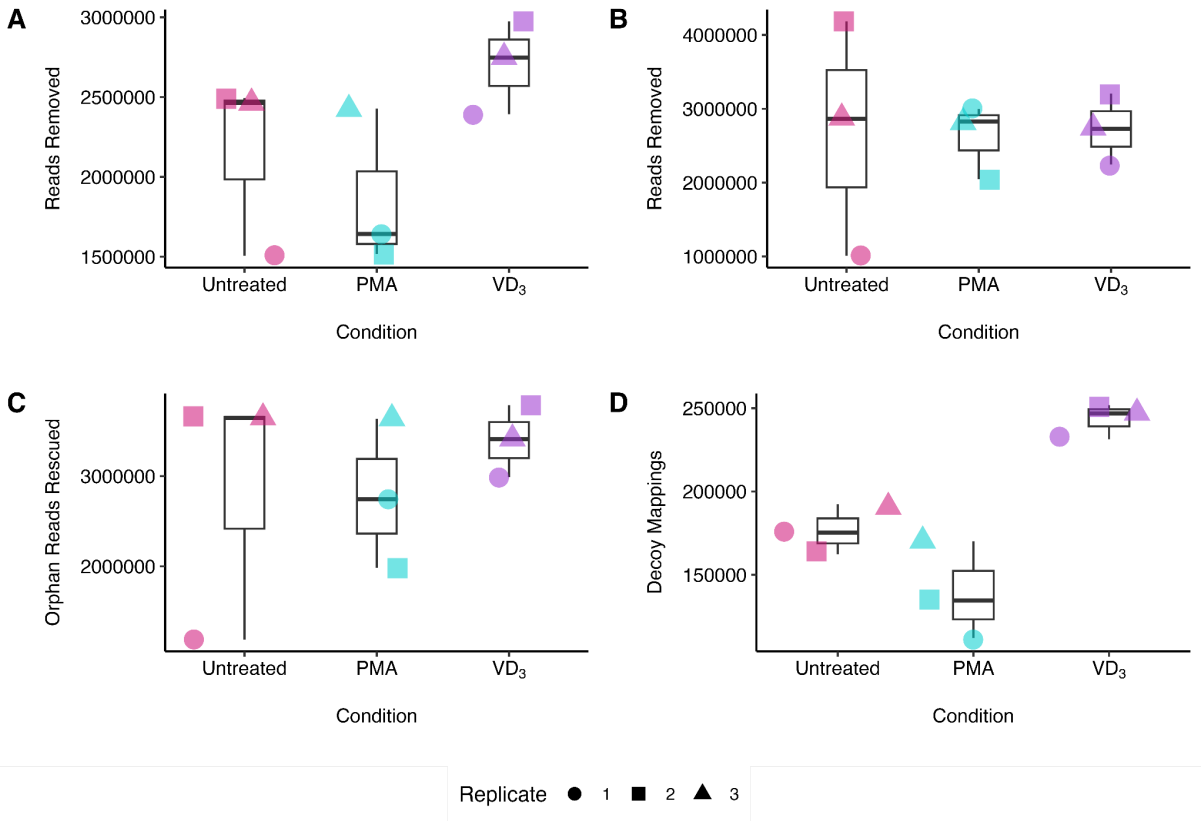

Figure 3.3: Sample read mapping and transcript abundance statistics. A) The number of reads removed for failing to meet the Salmon alignment threshold. B) The number of reads removed due to dovetail mappings. C) The number of orphan reads rescued. D) The number of reads mapped to the decoy transcripts that were excluded from downstream analyses.

The distribution of the TPM values across all samples and replicates was plotted in order to determine if the distribution was skewed by any extreme highly or lowly expressed features. This also allowed us to ensure that the samples were comparable with respect to library content (Figure 3.4). TPM values were found to be similar across all replicates within each treatment condition. The distribution of TPM values was also very similar across all treatment conditions. The TPM values for the genes encoding *CD14*, *CD16* (*FCGR3A*) and *CD36* were highlighted along the TPM distribution (Figure 3.4), as they were used as markers for the macrophage-like state, monocyte/macrophage state, and monocyte-like, respectively. Increased TPM values were observed for *CD14* (a marker for a macrophage-like state) in both VD_3-treated and PMA-treated samples, relative to untreated samples. However, it was noted that PMA-treated replicate 1 and untreated replicate 3 displayed results inconsistent with the other replicates in these treatment conditions. Similarly, inconsistencies were noted in the VD_3-treated samples,

where replicate 3 showed a difference with respect to *CD16* expression. Relative to replicates 1 and 2, replicate 3 of the VD_3-treated samples showed no expression of *CD16*. Furthermore, replicate 3 of the untreated samples displayed a marker expression pattern more consistent with VD_3-treatment, with respect to *CD16*.

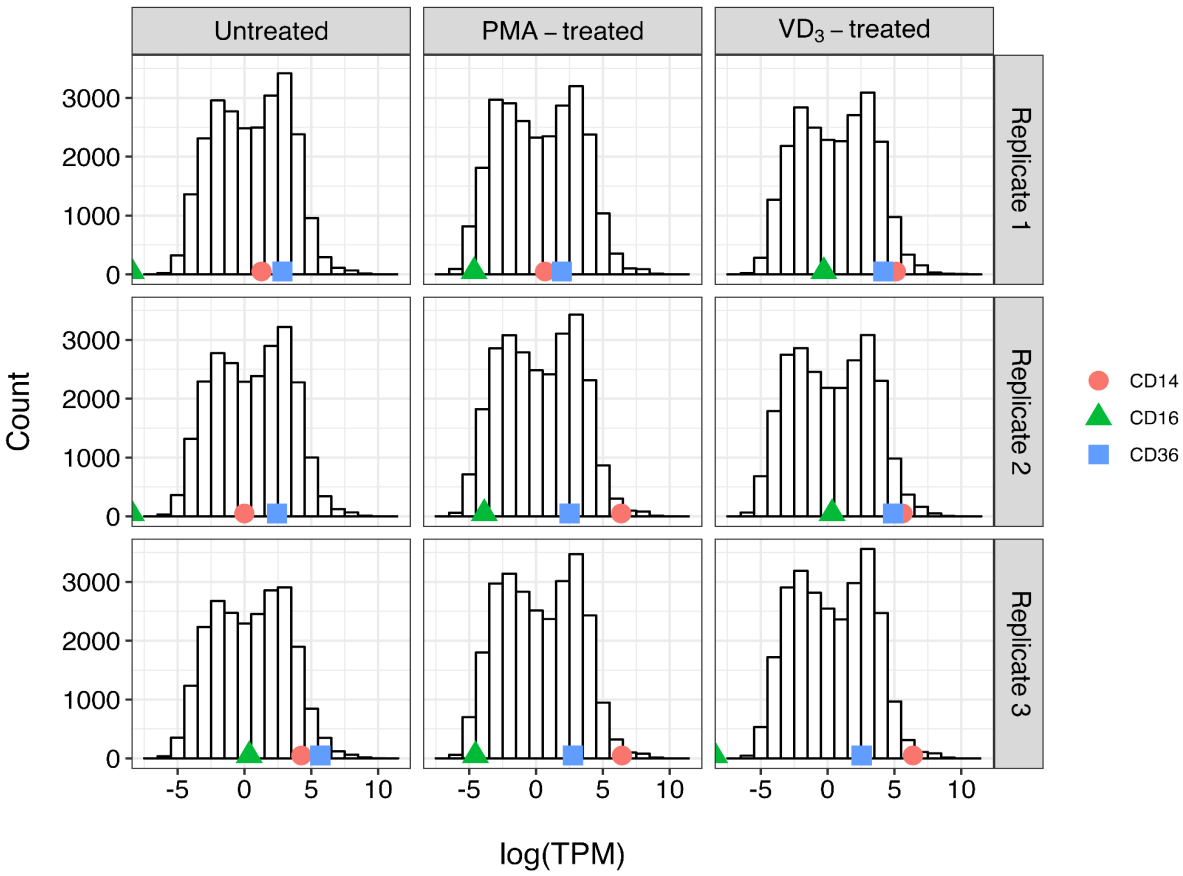

Figure 3.4: Distribution of TPM values per sample, across all treatment conditions. TPM values on the x-axis are plotted on a log-scale. The expression of the marker genes *CD14* (macrophage-like marker), *CD36* (monocyte-like marker), and *FCGR3A/CD16* (monocyte/macrophage marker) are indicated on the distribution for each sample. Untreated replicate 3 was inconsistent with replicate 1 and 2 of the same condition with regard to *CD16, CD14* and *CD36.* Similarly, VD_3-treated replicate 3 was inconsistent with its corresponding replicates with respect to *CD16* and *CD36*. PMA-treated replicate 1 was inconsistent with replicates 2 and 3 with respect to *CD14* expression.

3.3 Differential Gene Expression Analysis

The raw counts were normalised for sequencing depth and log-transformed (Figure S1), then further normalised with the regularised logarithmic DESeq2 function. Principal components analysis (PCA) of the transformed counts was performed, which showed clustering of samples predominantly based on treatment condition (Figure 3.5 and Figure 3.6), with 96% and 86% of the variance captured by the first principal component for PMA treatment and VD_3 treatment, respectively. Replicate 1 of the VD_3-treated samples was seen to cluster with replicates 1 and 2 of the untreated samples (Figure 3.5A). Additionally, replicate 3 from the untreated samples clustered with replicates 1 and 2 of the VD_3-treated samples. Based on this, and the inconsistencies seen, where replicate 1 from the untreated samples and replicate 3 for both the PMA and VD_3 samples showed inconsistent marker expression relative to their counterparts, replicate 3 of the untreated samples was excluded from further analyses. Similarly, PMA-treated replicate 1 was removed from further analysis due to this inconsistency in marker expression (Figure 3.4), despite clustering consistently with the other replicates in their treatment conditions during PCA (Figure 3.6A).

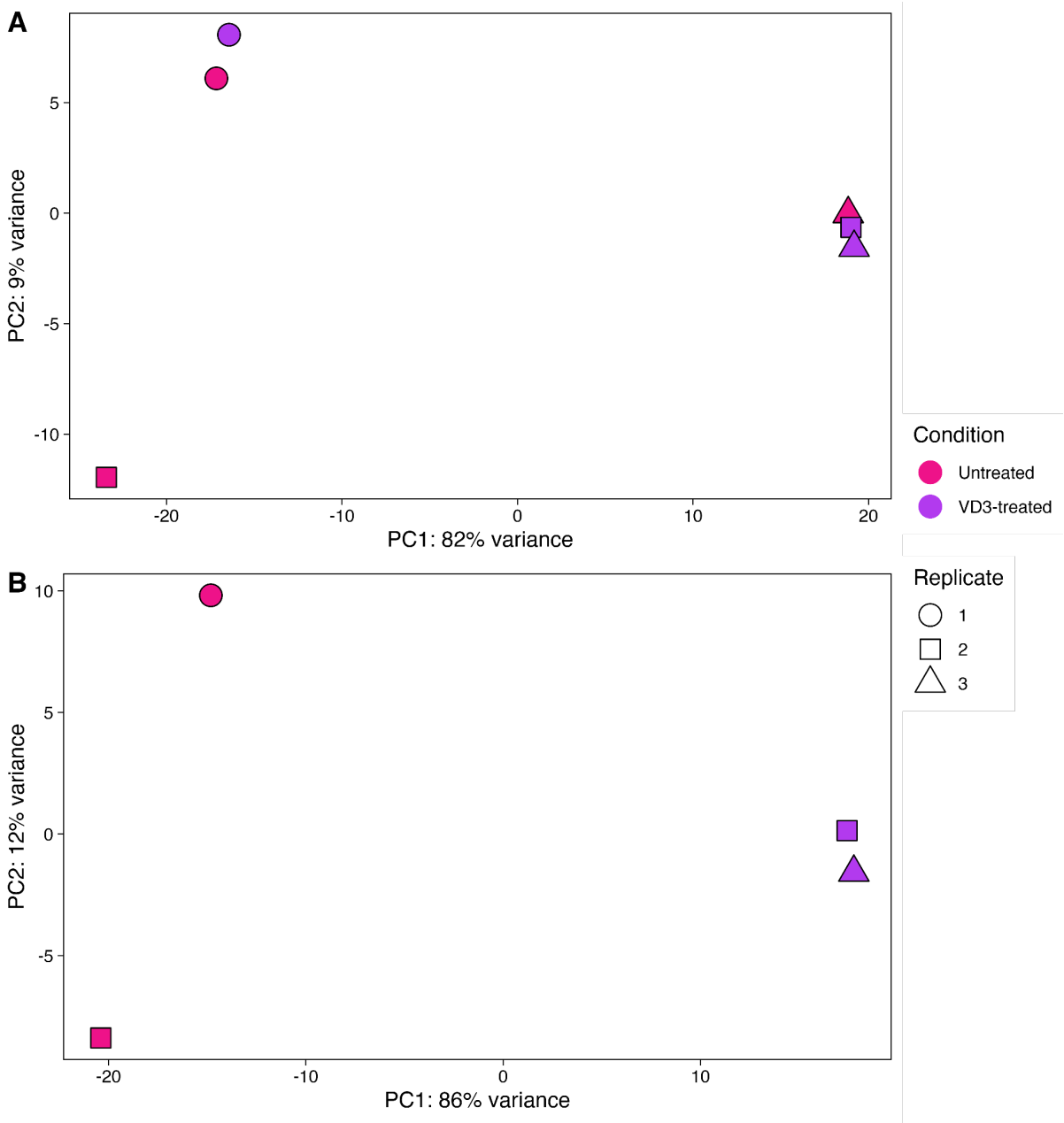

Figure 3.5: Principal Component Analysis (PCA) of VD_3-treated and untreated THP-1 samples following rlog normalisation. A) clustering of all available samples B) clustering of samples after replicate 1 of the VD_3-treated group and replicate 3 for the untreated group were removed from the analysis.

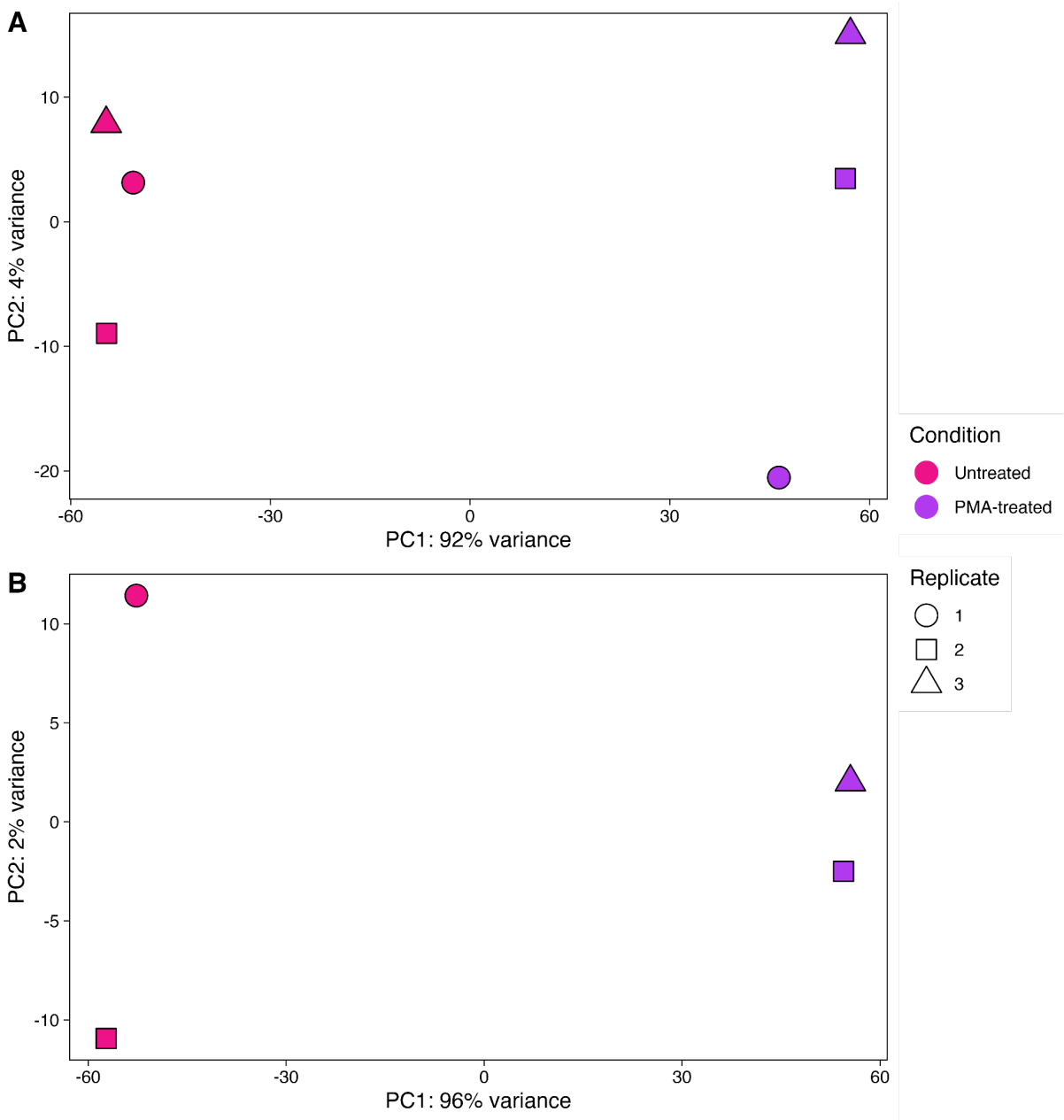

Figure 3.6: Principal Component Analysis (PCA) of PMA-treated and untreated THP-1 samples following rlog normalisation. A) clustering of all available samples B) clustering of samples after replicate 1 from the PMA-treated samples and replicate 3 from the untreated samples were removed from the analysis.

From the total of 17 504 genes analysed, differential gene expression analysis with DESeq2 revealed a total of 3 989 (22.79%) genes to be differentially expressed in response to PMA treatment (Figure 3.7A), relative to untreated THP-1 cells, while only 384 (2.19%) genes were found to be differentially expressed in response to treatment with VD_3 (Figure 3.7B). Following PMA treatment, more genes were found to be significantly down-regulated than up-regulated. However, the opposite was observed for VD_3 treatment, where more genes were significantly up-regulated than down-regulated. A total of 167 genes were found to be significantly differentially expressed in response to both PMA and VD_3 treatment (Figure 3.8A), 3 822 genes were found to be significantly differentially expressed in response to PMA treatment only, and 217 genes were found to be significantly differentially expressed in response to VD_3 treatment only (Figure 3.8A). Of the 167 DEGs identified in both treatments, 31 (18.56%) and 5 (3%) genes, respectively, were observed to be up-regulated and down-regulated irrespective of the treatment (i.e., differentially expressed in both) (Figure 3.8B). Furthermore, 37 (22.16%) of the 167 DEGs were up-regulated in PMA-treated cells and down-regulated in VD_3 treatment, and 94 (56.29%) were down-regulated as a result of PMA but up-regulated following VD_3 treatment (Figure 3.8B). From the 3 822 genes differentially expressed only as a result of PMA treatment, 1908 (49.92%) were down-regulated and 1914 (50.08%) were up-regulated (Figure 3.8C). From the 217 DEGs observed only as a result of VD3 treatment, 37 (17.05%) were down-regulated and 180 (82.95%) were up-regulated (Figure 3.8D).

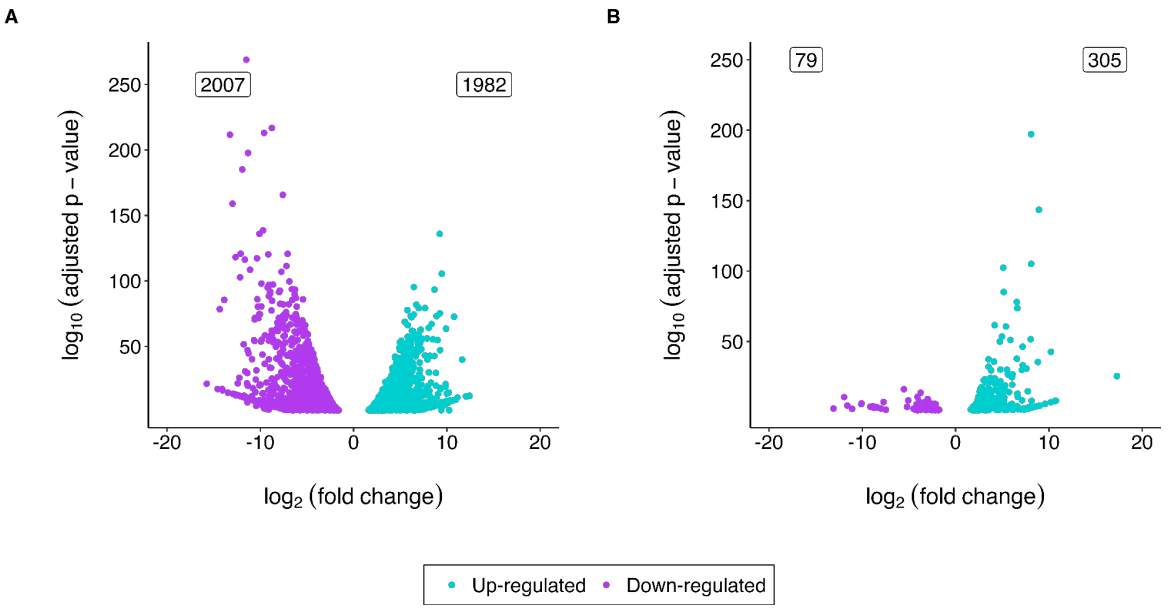

Figure 3.7: Volcano plot depicting the number of significantly up- and down-regulated genes identified in each treatment condition. A) genes significantly differentially expressed in response to PMA treatment and B) genes significantly differentially expressed in response to VD_3 treatment. Significance was determined with a threshold of an adjusted p-value < 0.05 and a $\log_2$(fold change) threshold of 1.

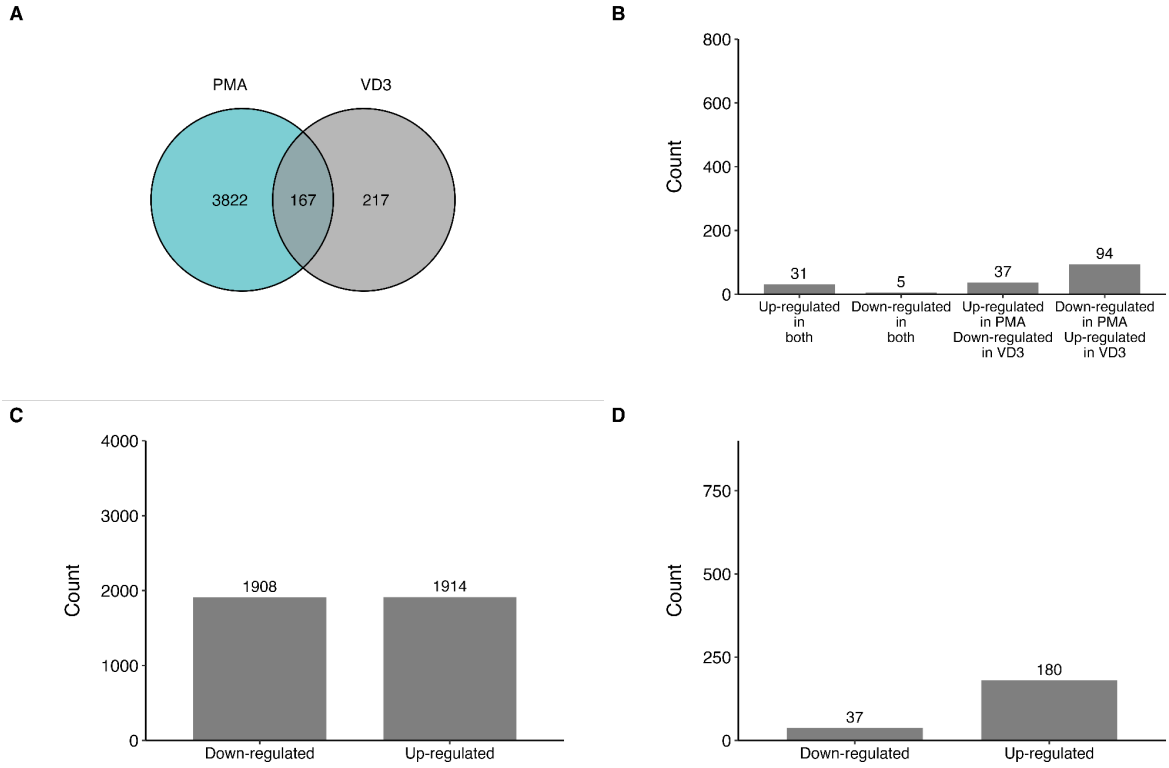

Figure 3.8: Differentially expressed genes unique to, and shared between, PMA and VD_3 treatment. A) The number of genes that were differentially expressed as a result of both treatments, and as a result of PMA treatment and VD_3 treatment individually. B) Of the genes differentially expressed as a result of both treatments, the number of genes expressed independent of treatment (i.e. up-regulated and down-regulated in both) were determined, as well as the number of genes that were differentially expressed in both treatments but in opposite directions (i.e., up-regulated in one and down-regulated in the other and vice versa). C) Of the genes differentially expressed as a result of PMA treatment only, the number of up- and down-regulated genes were determined. D) Of the genes differentially expressed as a result of VD_3 treatment only, the number of up- and down- regulated genes were determined. Significance was determined with a threshold of an adjusted p-value < 0.05 and a $\log_2$(fold change) threshold of 1.

3.4. *VDR* expression and VD_3 responsiveness

Given that PMA-treatment resulted in far more differentially expressed genes in the THP-1 cells compared to VD_3 treatment, the relative expression levels of *VDR* itself (to confirm expression) and that of two primary VDR target genes, cathelicidin anti-microbial peptide (*CAMP)* and cytochrome P450 family subfamily A member 1 (*CYP24A1)* (to confirm transactivation activity) were assessed. It was observed that, in VD_3-treated cells, VDR is expressed, however the change in expression relative to untreated cells was not significant. Furthermore, the relative expression of the VDR target genes, *CAMP* and *CYP24A1*, were shown to increase significantly in expression as a result of VD_3 treatment. No significant changes in expression of *VDR*, *CAMP* or *CYP24A1* was observed as a result of PMA treatment (Figure 3.9).

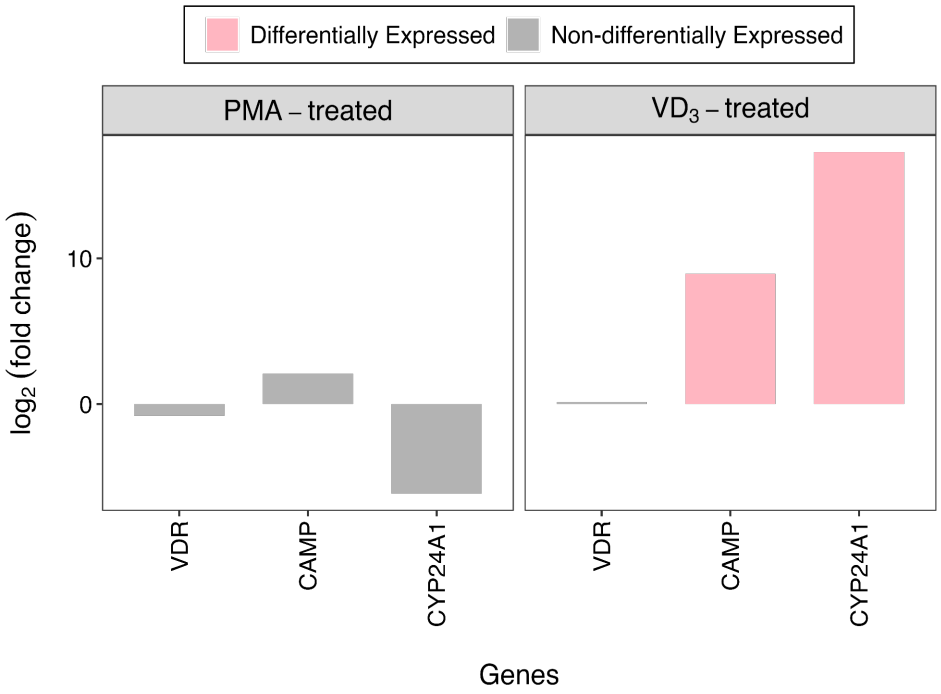

Figure 3.9: Relative expression levels of *VDR* and VDR target genes, *CAMP* and *CYP24A1*, as a result of PMA and VD_3 treatment. Significantly differentially expressed (adjusted p-value < 0.05 and log2(fold change) < |2|) and non-differentially expressed genes are depicted for each treatment.

3.5 Over-representation Analysis

The genes found to be significantly differentially expressed in response to treatment were used in an over-representation analysis using the enrichGO function provided in clusterProfiler v.4.0 (Wu *et al*., 2021). All significant GO terms are listed in Table S1.

3.5.1 Genes involved in myeloid differentiation

Following GO over-representation analysis, the myeloid leukocyte differentiation GO term was more closely analysed to identify the key genes involved in the differentiation process as a result of each treatment. The myeloid leukocyte differentiation GO term is the parent GO term that encompasses the monocyte and macrophage differentiation GO terms. The term contains 249 genes (Table S2), 67 of which were significantly differentially expressed in response to PMA treatment and five of which were significantly differentially expressed in response to VD_3 treatment (Figure 3.10). Transcription factor binding to IGHM enhancer 3 (*TFE3)*, *KIT* proto-oncogene and tribbles-1 (*TRIB1)* were found to be significantly differentially expressed in response to both treatments. Notably, *KIT* was up-regulated in PMA-treated cells but down-regulated in VD_3-treated cells. Ras association domain family member 2 (*RASSF2)* and peroxisome proliferator-activated receptor gamma coactivator 1-beta (*PPARGC1B*) were found to be differentially expressed in response to VD_3 treatment only, with an additional 64 genes being differentially expressed in response to PMA treatment only. Among the genes that were found to be significantly differentially expressed in response to PMA treatment were *CSF1*, *CSF-2* and *CSF-3* (Figure 3.10), which are known crucial players in the classically defined differentiation process. *CSF1*, *CSF-2* and *CSF-3* were not differentially expressed following VD_3 treatment (Figure 3.10). Furthermore, some of the key transcription factors known to be involved in the process of monocyte-to-macrophage differentiation were significantly differentially expressed in response to PMA treatment, but not VD_3 treatment (Figure 3.11). PMA treatment resulted in up-regulation of *CEBPA, GATA2* and *IRF8* and down-regulation of *CEBPB*, while VD_3 treatment showed no significant difference to the untreated control. Notably, PMA treatment did not result in changes in expression of *CEBPε, KLF2, KLF4* and *SPI1*.

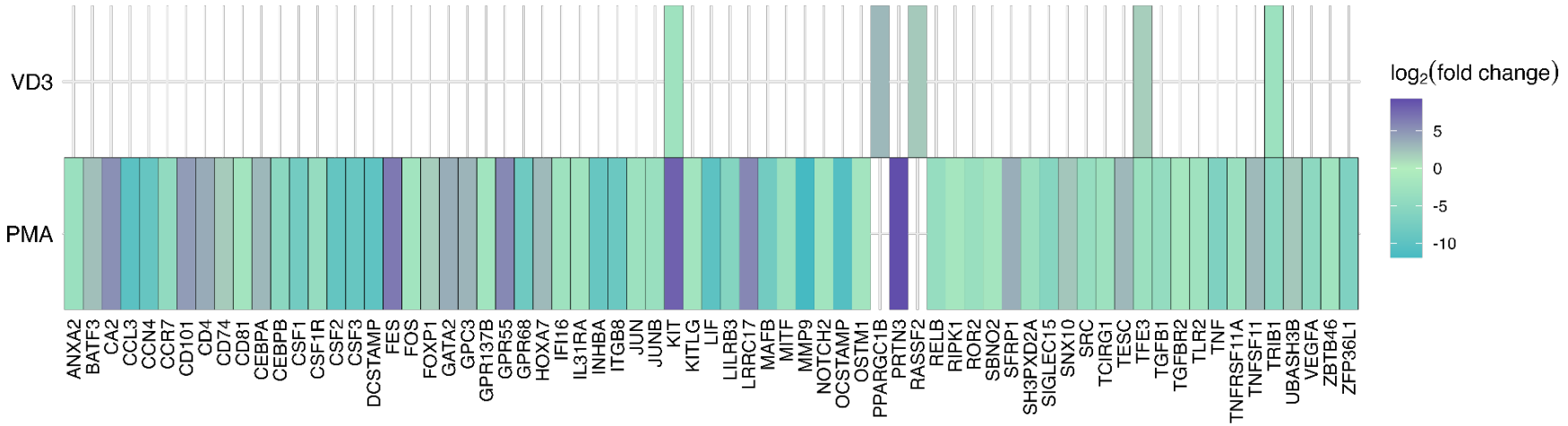

Figure 3.10: Genes within the GO term, myeloid differentiation, significantly differentially expressed in response to treatment with VD_3 and PMA. Blank regions indicate genes from the GO term that were not differentially expressed in response to either PMA or VD_3 treatment, while coloured-regions indicate the genes from the GO term that were significantly differentially expressed as a result of either treatment. The direction of the change in expression is depicted by the colour gradient of $\log_2$(fold change).

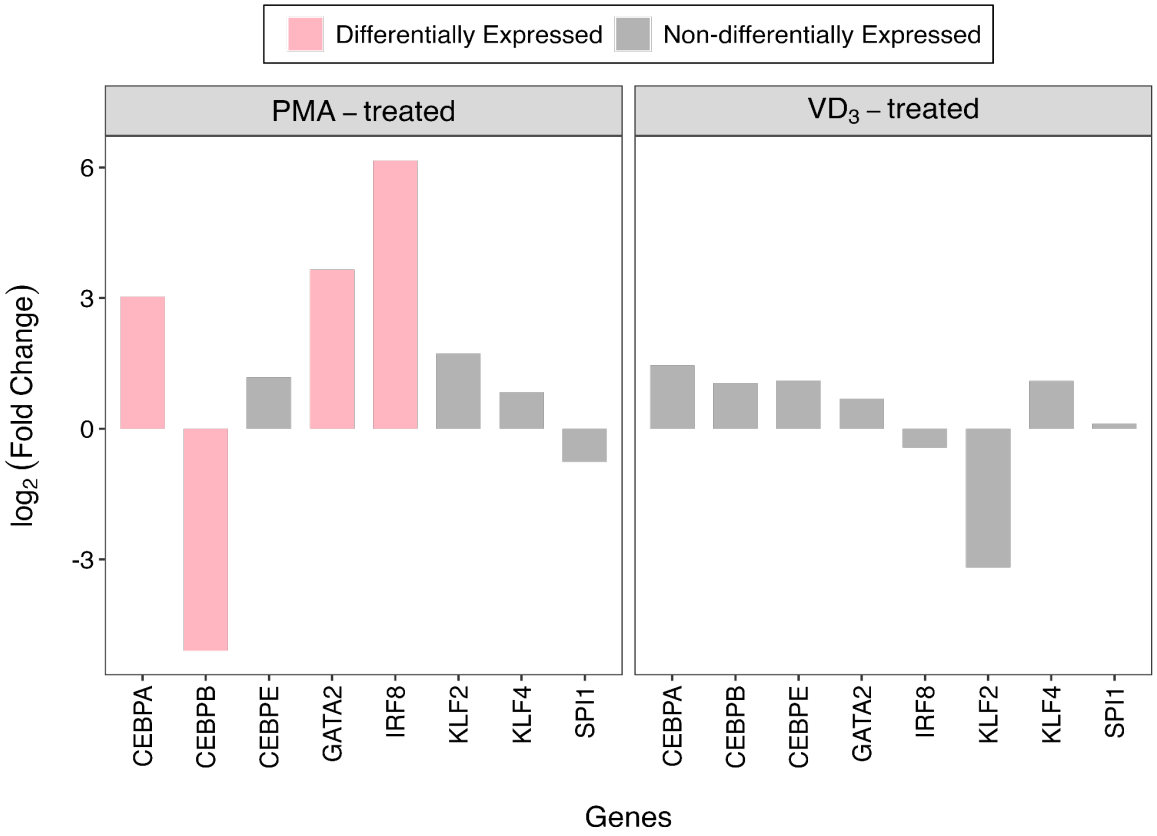

Figure 3.11: Changes in the expression levels of transcription factors known to be involved in monocyte-to-macrophage differentiation in response to treatment with PMA and VD_3. Significant differential expression (adjusted p-value < 0.05 and log2(fold change) < |2|) and non-differentially expressed transcription factor genes are depicted for each treatment.

3.5.2. Genes encoding monocyte- and macrophage-specific cell surface markers

To identify the stage of the differentiation process and characterise the maturity of the macrophage-state induced, monocyte and macrophage-specific cell surface markers were analysed. Enrichment analysis revealed significant down-regulation and up-regulation of *CD14* expression as a result of PMA and VD_3 (Figure 3.12) treatment, respectively. In addition, PMA treatment resulted in reduced expression of the *CD13* surface marker, as well as genes encoding the cytokines *TNF*, granulocyte-macrophage colony-stimulating factor (*GM-CSF)* and *M-CSF*. Significant up-regulation of human leukocyte antigen-DR (*HLA-DR)* and *CD64* was also observed as a result of PMA treatment (Figure 3.12), while not being differentially expressed

in VD_3-treated cells. Notably, no change in expression was observed in *CD33*, *CD116* and *CD123* as a result of PMA treatment.

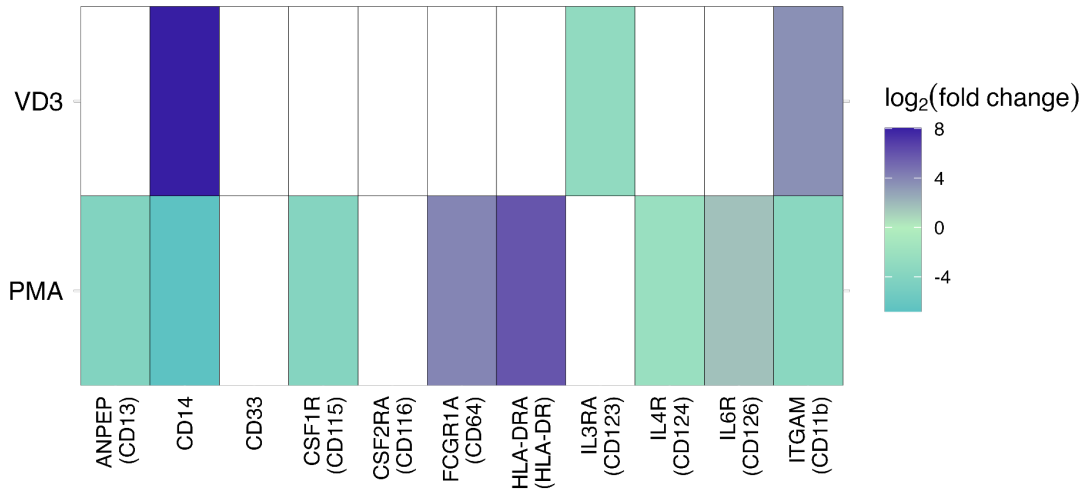

Figure 3.12: Genes encoding cell surface markers associated with macrophage differentiation that were significantly differentially expressed in response to PMA and VD_3 treatment. Blank regions indicate genes that were not significantly differentially expressed in response to treatment while coloured regions indicate the cell surface marker genes that were significantly differentially expressed as a result of either treatment. The direction of the change in expression is depicted by the colour gradient of log_2(fold change).

3.5.3 Genes involved in the response to Vitamin D_3

The 'response to vitamin D' GO term was also analysed in greater depth to determine the extent to which the VD_3 signalling pathway was activated as a result of the different treatments. This GO term contains 34 genes (Table S3), 11 of which were significantly differentially expressed in response to PMA treatment and two were significantly differentially expressed in response to VD_3 treatment. Notably, vitamin D receptor (VDR) is among the genes associated with this GO term (Table S3), but was not observed in Figure 3.13 as it was not differentially expressed in response to either treatment. Only two genes involved in this process were found to be significantly differentially expressed (up-regulated), following VD_3 treatment, namely

CYP24A1 and tenascin C (*TNC)* (Figure 3.13). These genes were not significantly differentially expressed in response to PMA treatment, but an overall pattern of significant down-regulation was observed in other genes involved in this process, such as plasma membrane calcium-transporting ATPase 1 (*ATP2B1), CYP27B1,* pim-1 proto-oncogene serine/threonine kinase *(PIM1),* secreted phosphoprotein 1 *(SPP1),* stanniocalcin-1 *(STC1),* stanniocalcin-2 *(STC2)* and tripartite motif containing 25 *(TRIM25)* in PMA-treated cells relative to untreated cells (Figure 3.13). Overall, it was found that there was no overlap in significantly differentially expressed genes within this GO term between the two treatment conditions.

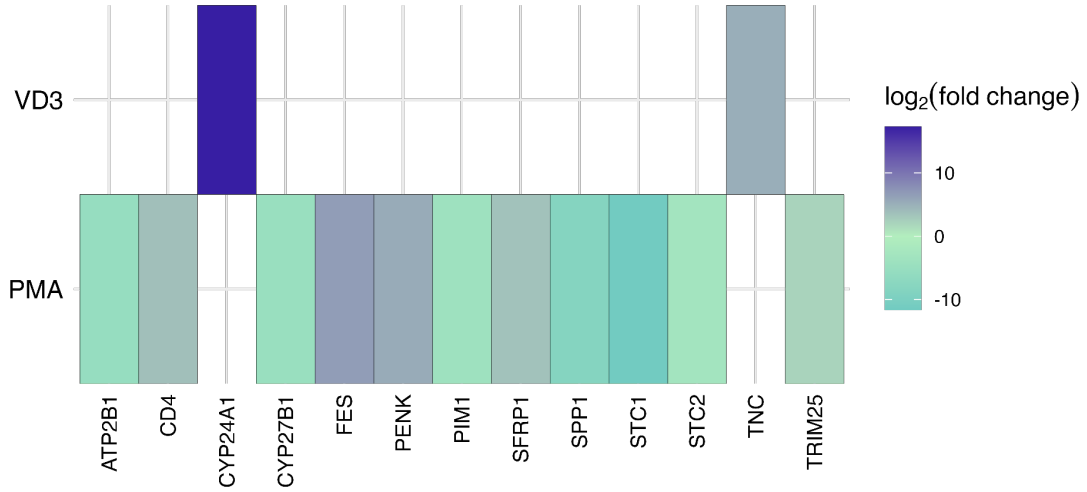

Figure 3.13: Genes within the GO term, response to vitamin D, significantly differentially expressed in response to treatment with VD3 and PMA. Blank regions indicate genes from the GO term that were not differentially expressed in response to either PMA or VD_3 treatment, while coloured-regions indicate the genes from the GO term that were significantly differentially expressed as a result of either treatment. The direction of the change in expression is depicted by the colour gradient of log_2(fold change).

3.5.4. Genes involved in the innate immune response

In order to determine the implications the different treatments would have for pathogen recognition, and therefore their relevance as a model system, the genes involved in the TLR signalling pathway were analysed. PMA treatment resulted in a change in the expression of multiple genes involved in the toll-like receptor (TLR) signalling pathway (Figure 3.14A), with notable decreases in the expression of *TLR1*, *TLR2,* and genes involved in pro-inflammatory immune responses (*TNFa*, *IL-1B* and *IL-6*). Significant down-regulation of *IL-8*, *RANTES* (regulated upon activation, normal T cell expressed and secreted), macrophage inflammatory protein-1 alpha (*MIP-1α)*, and macrophage inflammatory protein-1 beta (*MIP-1β)* was also observed. No significant changes in expression were observed for genes in this pathway in response to VD_3 treatment (Figure 3.14B), but VD_3 treatment resulted in significant up-regulation of *CD14*, which was significantly down-regulated in PMA treated cells.

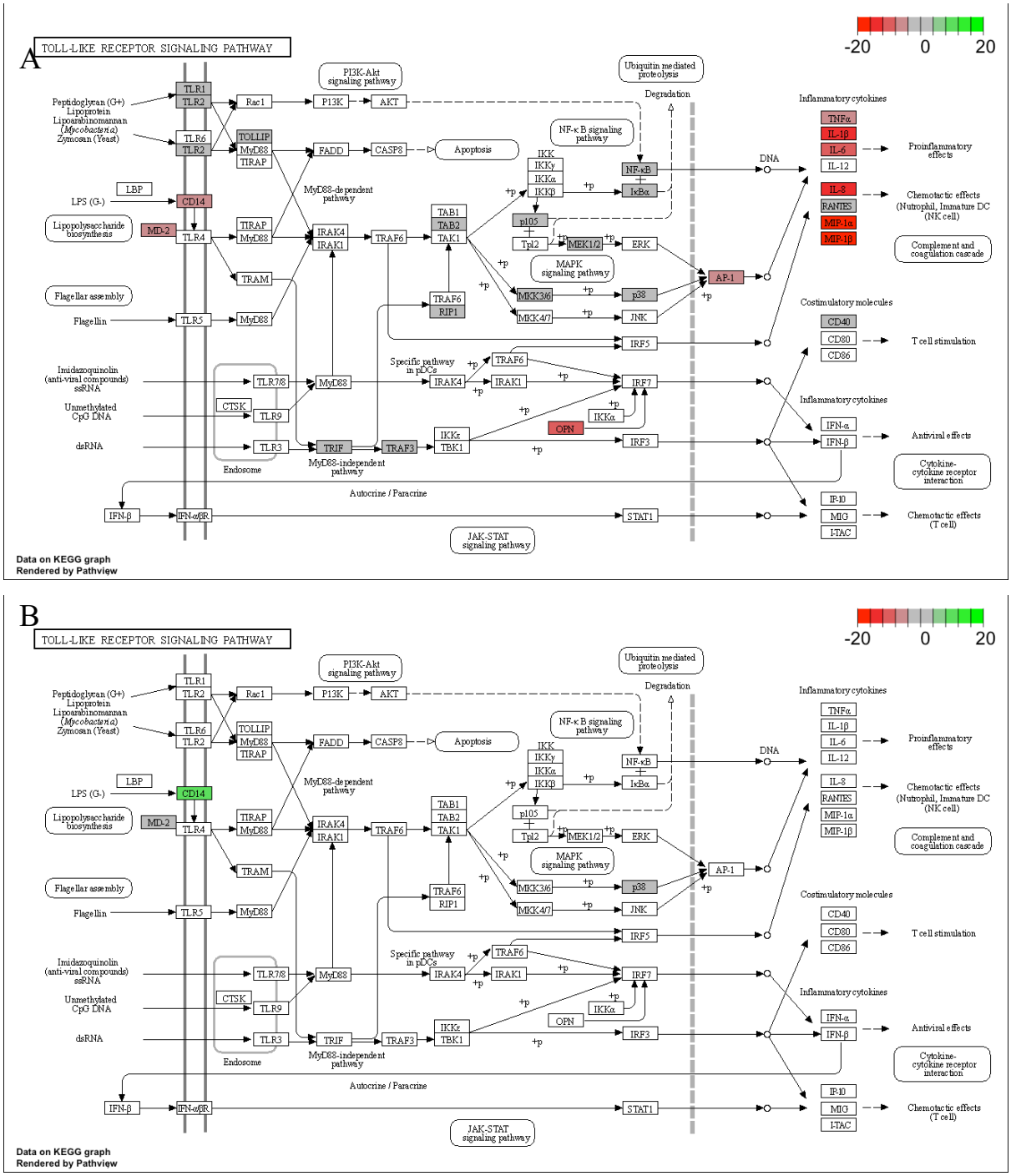

Figure 3.14: The toll-like receptor (TLR) signalling pathway. A) highlighting genes significantly differentially expressed in response to PMA treatment. B) highlighting genes significantly differentially expressed in response to VD_3 treatment. The direction of the change in expression is depicted by the $\log_2$(fold change) scale, with up-regulated (green) and down-regulated (red) genes shown.

Chapter 4: Discussion

PMA and VD_3 are known inducers of differentiation of promonocytic cell lines such as the THP-1 cell line. As such, these agents are used in THP-1 cells to model monocyte-to-macrophage differentiation. This study compared THP-1 cells treated with each of these agents to an untreated state and identified genes that were significantly differentially expressed as a result of these treatments. PMA treatment resulted in more changes in expression relative to VD_3 treatment. The DEGs were assessed in terms of whether they were unique to either treatment or expressed as a result of both treatments. Furthermore, the involvement of these differentially expressed genes in specific pathways was analysed to determine the key players involved in shifting the cells toward a macrophage-like state in each treatment. Apart from a few genes observed to be crucial to the process of differentiation, irrespective of treatment, the treatments were observed to largely involve different biological pathways, resulting in cells that were phenotypically distinct from each other at the transcriptional level. This included changes observed in the expression of genes encoding transcription factors known to be involved in the differentiation process, as well as those encoding surface markers representative of monocytes and macrophages.

4.1. Key Players in the Differentiation Process

Genes associated with myeloid differentiation that were differentially expressed as a result of both treatments were used to determine common genes responsible for the movement of the cells toward a macrophage-like phenotype. These genes included *TFE3*, *KIT* and *TRIB1*. *TFE3* is from a family of basic helix-loop-helix leucine zipper transcription factors (Steingrimsson *et al.*, 2002). TFE3 has been associated with the differentiation of monocytes into macrophages in U937 and HL-60 cells treated with PMA (Zanocco-Marani *et al.*, 2006). Another study done by Zanocco-Marani and colleagues further outlined that TFE3 acts as a regulator for the transcription factor, MAFB (Zanocco-Marani et al., 2009). Several studies have reported *MAFB* expression to trigger macrophage differentiation with resulting end states showing a reduced monocyte and DC phenotype (Sieweke *et al.*, 1996; Bakri *et al.*, 2005; Gemelli *et al.*, 2006). Zanocco-Marani *et al*., (2009) showed that *MAFB (basic leucine zipper transcription factor)* increases in expression, but to a lesser extent, in the presence of *TFE3* during differentiation, however the associated time-point of the differentiation process was not

reported. We observed a significant decrease in the expression of *TFE3* as a result of both treatments, and furthermore, *MAFB* was down-regulated following PMA treatment and not differentially expressed as a result of VD_3 treatment.

These findings were inconsistent with the claim that *MAFB* and *TFE3* increase upon PMA stimulation. This inconsistency may be attributed to a number of factors. *TFE3* expression was measured in HL-60 and U937 after 36 hours of PMA treatment (Zanocco-Marani *et al.*, 2006), while this study observed *TFE3* expression in THP-1 cells following 72 hours of PMA treatment. It is plausible that the cells in our study have surpassed the stage of differentiation where *TFE3* increases and are indicative of a more mature macrophage-like state. In addition, this study utilised data where the PMA concentration used to induce differentiation was higher and this likely influences the result observed. In addition, with respect to *MAFB* expression, it is important to note that while *MAFB* expression is associated with the process of differentiation, its inactivation does not prevent differentiation (Gemelli *et al.*, 2006). This supports the notion that the process of differentiating monocytes into macrophages is governed by a host of transcription factors. The role of *TFE3* in the differentiation process, outlined in various studies and the fact that its expression was seen to reduce as a result of both treatments in this study, suggests that *TFE3* is a common and key gene associated with the differentiation of monocytes into macrophages and that this expression is likely influenced by treatment time and concentration.

Another gene that was observed as differentially expressed (down-regulated) as a result of both treatments was *TRIB1*. TRIB1 is a pseudokinase that aids in the control of signalling pathways such as the mitogen activated protein kinases (MAPK) and PI3-kinase pathway. *TRIB1* is a key oncogene in acute myeloid leukaemia (Röthlisberger *et al.*, 2007; Yoshida *et al.*, 2013) and has been shown to play an key role during the differentiation of M2 macrophages in early atherosclerosis (Satoh *et al.*, 2013), as well as in prostate cancer (Liu *et al.*, 2019). The latter study assessed the effect TRIB1 had on the differentiation of THP-1 cells within a tumorigenic microenvironment following co-culturing with prostate cancer cells. TRIB1 may, therefore, be a key player in the differentiation of monocytes into macrophages, and may even play a role in macrophage polarisation. However, the extent to which it is involved in this process, specifically in THP-1 cells, is not yet entirely clear.

Genes known to be involved in myeloid differentiation and observed to be differentially expressed only in response to VD_3 treatment include *RASSF2* and *PPARGC1B*. *RASSF2* is a VD_3 target gene (Warwick *et al.*, 2021), however the link between the gene and myeloid differentiation is unknown. Additionally, with respect to *PPARGC1B*, an epigenetic study performed by Seuter *et al.* (2013) classified *PPARGC1B* as an early VDR target gene with dynamic chromatin opening. This means that *PPARGC1B* may be a gene unique to VD_3 treatment that plays a key role in the differentiation process. Furthermore, PU.1, a pioneer transcription factor known to be involved in the monocyte-to-macrophage differentiation process, has been shown to be relevant to the transcriptional activation of VDR target genes such as *PPARGC1B*, where reduced PU.1 expression was associated with reduced *PPARGC1B* expression (Seuter *et al.*, 2017). We observed no change in expression in the gene encoding PU.1 (*SPI1*) and down-regulation of *PPARGC1B*. While this may suggest a role for *PPARGC1B* expression in the differentiation process induced by VD_3, independent of PU.1 expression, it is also likely that at this time point, *SPI1* has returned to baseline levels of expression.

In keeping with the expression patterns of transcription factors known to be involved in the monocyte-to-macrophage differentiation process, VD_3 treatment did not result in significant changes in gene expression of any of the factors assessed in this study. These include CEBPα (Reddy *et al.*, 2002), CEBPβ (Yang *et al.*, 2000), GATA2 (Walsh *et al.*, 2002), IRF8 (Meraro *et al.*, 1999), and PU.1. Of these transcription factors, VD_3 activity has previously been associated with regulation of CEBPα and PU.1. Through its interaction with transcription factors such as PU.1 and CEBPa, VDR has been shown to increase the chromatin accessibility of the enhancer regions that it binds to in its ligand-activated state (Nurminen *et al.*, 2019; Seuter *et al.*, 2017). Our findings showed no significant changes in the expression of these transcription factor genes. This suggests that VD_3-induced differentiation likely occurs by means of a process dependent on the expression of these transcription factor genes at an earlier time point and after treatment for 72 hours this expression has returned to baseline levels.

With respect to changes in the expression of transcription factors known to be involved in the differentiation process observed following treatment with PMA, *CEBPα* and *GATA2* were seen to increase in expression, with no difference in expression observed in *PU.1/SPI1*. PU.1 has been found to inhibit GATA-2 at the protein-level (Zhang *et al.*, 1999) and PU.1-mediated

down-regulation of *GATA-2* expression has been shown to commit myeloid progenitors toward macrophage differentiation (Walsh *et al.*, 2002). In addition to this, *CEBPα* expression has been associated with blocking of differentiation into macrophages in the U937 promyelocytic cell line (Radomska *et al.*, 1998), as it has the ability to interfere with the transcriptional activity of PU.1 (Reddy *et al.*, 2002). Dahl *et al.*, (2003) demonstrated that at the protein-level, the relative concentration of PU.1 to CEBPα has the ability to determine commitment to either a macrophage or neutrophil cell fate. They further showed that CSF-3 plays a role in this decision by up-regulating *CEBPα* and shifting the cells away from a macrophage fate. These findings were not all consistent with what we observed at the gene expression level, where *CEBPα* increased in expression (opposite to what was expected) while *CSF-3* was seen to decrease in expression, following PMA treatment.

A study done by Gažová *et al*., (2020) demonstrated fairly constant expression of *PU.1/SPI1* in THP-1 cells over a period of 96 hours, after treatment with 48.6 nM PMA, with notable peaks in expression during the 8-10 hour timepoints. This was not consistent with what was observed in this study, as *PU.1/SPI1* was observed to have no significant change in expression following 72 hours of treatment with 500 nM PMA. While the PMA concentration may be at the core of this difference, the findings of Gažová *et al*., (2020) suggests that the process of differentiation induced by PMA is not linear. Instead, it likely involves a cascade of transiently up- and down-regulation of the expression of genes that encode known transcription factors (Gažová *et al.*, 2020). Therefore, the inconsistencies observed in the expression of the known transcription factors associated with differentiation, assessed in this study, may be indicative of expression at an alternate stage of the differentiation processes, where the resulting state is independent of PU.1 and *GATA-2* and *CEBPα* is transiently up-regulated.

The treatments also showed distinct differences in the expression of traditional monocyte and macrophage cell surface markers. The monocyte-surface marker gene, *CD14*, is down-regulated during differentiation of primary monocytes into macrophages (Steinbach and Thiele, 1994). *CD14* expression in PMA-treated THP-1 cells was consistent with primary cells in this regard. VD_3-treated cells, however, showed increased expression of *CD14*. This increase in *CD14* expression was consistent with findings from studies using VD_3 as a differentiation inducing agent in other monocytic cell lines (Sadeghi *et al.*, 2006; Daigneault *et al.*, 2010;). The up-regulation of *CD14* due to VD_3 and the down-regulation of *TLR2* expression as a result

of PMA treatment was found to be consistent with what has previously been reported when differentiating primary monocytes into macrophages (Daigneault *et al.*, 2010; Henning *et al.*, 2008; Steinbach and Thiele, 1994). A notable up-regulation of *CD64* was also observed in PMA-treated cells. *CD64* is constitutively expressed on monocytes and macrophages (Akinrinmade *et al.*, 2017) and according to Hristodorov *et al.*, (2015) CD64 increases in expression on the surface of macrophages that are polarised toward the M1 phenotype. This reinforces the notion that PMA treatment is shifting the cells toward a macrophage-like phenotype.

The differing patterns of expression observed in myeloid differentiation genes and transcription factors for both treatments indicate that while there are a few common changes in gene expression, different processes are being initiated and utilised by the different treatments. These findings further indicate that the macrophage-like cell states resulting from the different treatments induce distinct expression patterns from each other. It is made clear that while the state induced by PMA involves changes in many of the myeloid differentiation associated genes and known transcription factor genes, it is not representative of all characteristics of a macrophage. Furthermore, it is clear that VD_3 treatment did not result in significant changes in what can be defined as a classically characterised process of myeloid differentiation and is associated with fewer characteristics and expression patterns consistent with a macrophage.

4.2. VD_3 Response and The Mechanism of Differentiation Induced by VD_3

VDR was not differentially expressed as a result of VD_3 treatment. While this was not consistent with findings that VDR increases in expression upon VD_3 stimulation (Pramanik *et al.*, 2004), it did not indicate a lack of response to VD_3 by the cell, as significant up-regulation was observed in the VDR downstream target genes, *CAMP* and *CYP24A1*. It has been shown that expression of the receptor is tightly controlled, and an increase in expression is not always observed upon stimulation (Tulk *et al.*, 2015). Therefore, we can deduce that the VDR pathway is, in fact, activated following VD_3 treatment at the tested concentration. However, due to the concentration of the VD_3 used in this study likely being too high, a negative feedback loop may have been triggered in an effort to maintain homeostasis. VD_3 levels are carefully regulated in a negative feedback loop, where VD_3 inhibits 1-α-hydroxylase (CYP27B1) while also stimulating 24-hydroxylase enzymes (CYP24A1), which is consistent with our observations.

This ensures that VD_3 levels are maintained within a limited range and prevents excessive VD_3 signalling (Aranow, 2011). Therefore, it may be that the concentration of the VD_3 used in this study resulted in inhibition, rather than activation, of this response.

VDR has previously been shown to act together with PU.1 and CEBPα to regulate myeloid differentiation (Barragan *et al.*, 2015). However, the observed expression pattern of key transcription factors associated with monocyte-to-macrophage differentiation, as well as that of other genes characterised as key players in the process, provided the impression that VD_3 treatment likely activates a different cascade of pathways to those induced by PMA treatment. Tenascin C (TNC) was differentially expressed as a result of VD_3 treatment. The glycoprotein encoding gene has been found to be inhibited by VD_3 in mammary epithelial cells (González-Sancho *et al.*, 1998), however this is inconsistent with the up-regulation of the gene we observed, which may be attributed to the VD_3 concentration. TNC has also been identified as an endogenous modulator that is able to promote the polarisation of macrophages toward a M1 phenotype. This is based on the ability of TNC to induce the production of pro-inflammatory cytokines through TLR4 (Yalcin *et al.*, 2020). This suggests a link between *TNC* and VD_3, as well as the macrophage phenotype, and that *TNC* expression may be a factor contributing to the shift in cell state to one more representative of a macrophage following VD_3 treatment.

4.3. Implications for Pathogen Recognition

Genes involved in the TLR signalling pathway were shown to be significantly down-regulated in response to PMA treatment. Changes in the expression of genes in this pathway may have important implications for pathogen recognition when using this cell line and these treatments as the experimental system. A previous study (Sadeghi *et al.*, 2006) reported that treatment with VD_3 resulted in a reduction in *TLR2* and *TLR4* expression and suggested that the impaired response to bacterial PAMPs observed in monocytes treated with VD_3 may be, in part, due to this down-regulation. However, no change in *TLR2* and *TLR4* expression in response to treatment with VD_3 was observed in this study. This may have been due to the mentioned concentration of the reagent used in this study or different time periods of treatment. Down-regulation of *TLR1* and *TLR2* was also observed following PMA treatment. This may also have implications for the detection of viral PAMPs, as human cytomegalovirus (HCMV) has been shown to induce an inflammatory response through TLR2 (Compton *et al.*, 2003).

4.4. Implications for Cytokine Production

A reduction in the expression of genes encoding pro-inflammatory cytokines was seen as a result of PMA treatment. While this is not what we expected to see with respect to *TNFα*, *RANTES*, and *MIP1β*, which have been seen to increase in a time and concentration dependent manner (Park *et al.*, 2007), reduced IL-1β expression is characteristic of the shift from a monocyte-like state to that more representative of a macrophage (Awad *et al.*, 2017). Upon stimulation, IL-1β is also known to increase the expression of TNFα (Jayaraman *et al.*, 2013) and mediate the recruitment of additional pro-inflammatory factors such as IL-6, MIP1α, MIP1β (Jayaraman *et al.*, 2010, 2013). This suggests that the reduction in expression of proinflammatory genes in the cell state resulting from PMA treatment, may be IL-1β-mediated. However, this would have to be confirmed through experimental studies. In addition, no changes in expression were observed in cytokine-encoding genes following VD_3 treatment. A host of studies has observed VD_3 treatment of THP-1 cells to result in an anti-inflammatory phenotype (Matilainen *et al.*, 2010; Yang *et al.*, 2012; Wang *et al.*, 2014). This has been found to be the case in human monocytes and macrophages as well (Di Rosa *et al.*, 2012; Du *et al.*, 2009). Interestingly, a study performed by Tulk *et al.*, (2015) observed an IL-1β-mediated proinflammatory phenotype after stimulating PMA-differentiated THP-1 cells with VD_3. Based on this, together with our findings, the effect that the treatments have on the cells' cytokine production capacity is inconsistent and unclear with respect to previous studies. This indicates the need for caution when deciding on a treatment.

4.5 Study Limitations

Gene expression can be affected by a number of internal and external factors and therefore differential gene expression studies are not without limitations. Inconsistencies in the sequencing data resulted in the removal of a replicate from each treatment condition as well as the untreated samples. As such, the differential gene expression analysis was performed with only two replicates per condition. While the tools used in this analysis take such factors into consideration, this reduces the sensitivity of the analysis. In addition, conclusions in this study can only be drawn from relative changes in gene expression at the concentrations and time points tested.

4.6. Conclusions

This study characterised transcriptional changes induced in THP-1 cells when treated with PMA and VD_3 in order to bring about differentiation into a macrophage-like state. While there are common genes involved in both processes, such as *TFE3*, *KIT* and *TRIB1*, treatment of THP-1 cells with PMA and VD_3 largely involve different biological pathways and resulted in cells that were phenotypically distinct from each other at the transcriptional level. PMA appeared to induce a macrophage-state representative of one at a different stage in the differentiation process relative to VD_3 treatment. This was based on the cell surface marker expression, as well as expression of genes that are known to be key players in what can be defined as the "classical", well characterised process of differentiation. Furthermore, PMA-induced differentiation resulted in changes in a large number of the genes involved in this differentiation process, whereas VD_3 did not. While it became clear that the cell states resulting from the different treatments did share some characteristics with macrophages, with respect to cell surface markers and transcription factor gene expression, they cannot be completely classified as macrophages, as there are core differences in the states induced between the different agents, as well as relative to what is expected of human macrophages. Genes such as *TFE3, KIT* and *TRIBI* may act as potential common key players within the differentiation process of THP-1 cells, irrespective of treatment. Furthermore, key differences observed in the expression of genes encoding pathogen recognition receptors and cytokines suggest that the differentiation-inducing agent used may have important implications for these cells' capacity to recognise pathogens and produce cytokines. The findings of this study therefore emphasise that it is crucial to carefully consider the choice of differentiation-inducing agent when using THP-1 cells as an experimental system for studying monocyte-to-macrophage differentiation.

4.7 Future Work

In characterising the transcriptional changes resulting from treatment of THP-1 cells with different differentiation-inducing agents, the findings from this work suggest that factors need to be considered when choosing which cell line is appropriate for functional studies. Computationally, the findings in this study can benefit from the incorporation of additional omics studies. However, with respect to validating these findings experimentally, future work should include protein-level studies to determine if these differences and commonalities, with respect to the PMA and VD_3 treatments, are observed at this level in THP-1 cells. Furthermore,

different concentrations of the inducing agents should be assessed. This would confirm the findings of this study and aid in characterising the agents as differentiation-inducers. In turn, this would provide markers specific to the THP-1 model system that can be referenced when deciding on and utilising a differentiation-inducing agent.

Appendices and Supplementary Data

Supplementary Figures and Tables

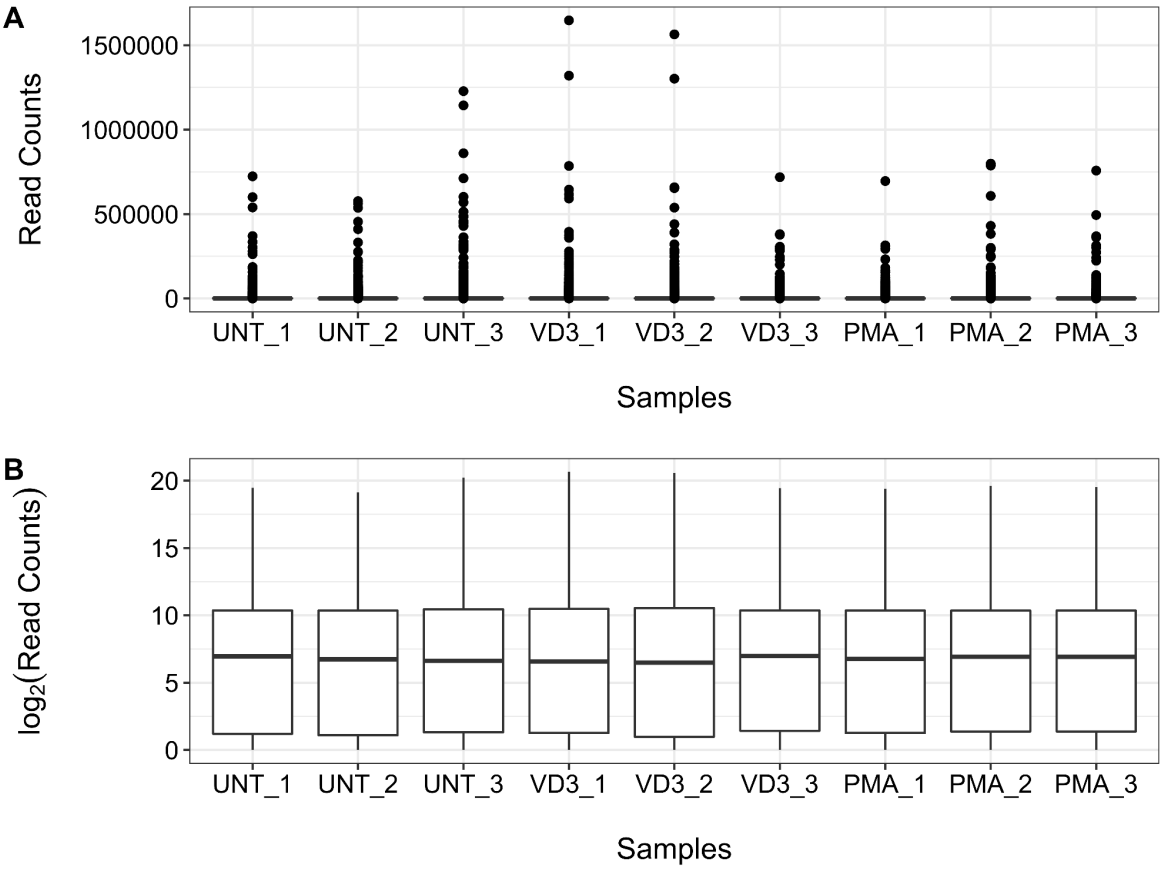

Figure S1: Distribution of normalised read counts per sample. A) Raw sequencing read counts were normalised for differences in sequencing depth. B) The normalised counts were further log_2-transformed.

Table S1: All Significant GO Terms Determined by Over-representation Analysis for PMA and VD_3-treated cells

Overrepresentation Results

Table S2: All Genes Associated with the GO term, Myeloid Leukocyte Differentiation

GO: 0002573 Myeloid Leukocyte Differentiation

Table S3: All Genes Associated with the GO term, Response to Vitamin D

GO: 0033280 Response to Vitamin D

References

Aird, D., Ross, M.G., Chen, W.-S., Danielsson, M., Fennell, T., Russ, C., Jaffe, D.B., Nusbaum, C., Gnirke, A., 2011. Analyzing and minimizing PCR amplification bias in Illumina sequencing libraries. Genome Biol 12, R18. https://doi.org/10.1186/gb-2011-12-2-r18

Akashi, K., Traver, D., Miyamoto, T., Weissman, I.L., 2000. A clonogenic common myeloid progenitor that gives rise to all myeloid lineages. Nature 404, 193–197. https://doi.org/10.1038/35004599

Akinrinmade, O.A., Chetty, S., Daramola, A.K., Islam, M., Thepen, T., Barth, S., 2017. CD64: An Attractive Immunotherapeutic Target for M1-type Macrophage Mediated Chronic Inflammatory Diseases. Biomedicines 5, 56. https://doi.org/10.3390/biomedicines5030056

Akira, S., Uematsu, S., Takeuchi, O., 2006. Pathogen Recognition and Innate Immunity. Cell 124, 783–801. https://doi.org/10.1016/j.cell.2006.02.015

Alder, J.K., Georgantas, R.W., Hildreth, R.L., Kaplan, I.M., Morisot, S., Yu, X., McDevitt, M., Civin, C.I., 2008. Kruppel-Like Factor 4 Is Essential for Inflammatory Monocyte Differentiation In Vivo. The Journal of Immunology 180, 5645–5652. https://doi.org/10.4049/jimmunol.180.8.5645

Aranow, C., 2011. Vitamin D and the Immune System. J Investig Med 59, 881–886. https://doi.org/10.231/JIM.0b013e31821b8755

Ashburner, M., Ball, C.A., Blake, J.A., Botstein, D., Butler, H., Cherry, J.M., Davis, A.P., Dolinski, K., Dwight, S.S., Eppig, J.T., Harris, M.A., Hill, D.P., Issel-Tarver, L., Kasarskis, A., Lewis, S., Matese, J.C., Richardson, J.E., Ringwald, M., Rubin, G.M., Sherlock, G., 2000. Gene ontology: tool for the unification of biology. The Gene Ontology Consortium. Nat. Genet. 25, 25–29. https://doi.org/10.1038/75556

Atri, C., Guerfali, F.Z., Laouini, D., 2018. Role of Human Macrophage Polarization in Inflammation during Infectious Diseases. Int J Mol Sci 19. https://doi.org/10.3390/ijms19061801

Auwerx, J., 1991. The human leukemia cell line, THP-1: a multifacetted model for the study of monocyte-macrophage differentiation. Experientia 47, 22–31. https://doi.org/10.1007/bf02041244

Awad, F., Assrawi, E., Jumeau, C., Georgin-Lavialle, S., Cobret, L., Duquesnoy, P., Piterboth, W., Thomas, L., Stankovic-Stojanovic, K., Louvrier, C., Giurgea, I., Grateau, G.,

Amselem, S., Karabina, S.-A., 2017. Impact of human monocyte and macrophage polarization on NLR expression and NLRP3 inflammasome activation. PLOS ONE 12, e0175336. https://doi.org/10.1371/journal.pone.0175336

Babraham Bioinformatics - FastQC A Quality Control tool for High Throughput Sequence Data [WWW Document], n.d. URL https://www.bioinformatics.babraham.ac.uk/projects/fastqc/ (accessed 4.23.20).

Bakri, Y., Sarrazin, S., Mayer, U.P., Tillmanns, S., Nerlov, C., Boned, A., Sieweke, M.H., 2005. Balance of MafB and PU.1 specifies alternative macrophage or dendritic cell fate. Blood 105, 2707–2716. https://doi.org/10.1182/blood-2004-04-1448

Balakrishnan, R., Harris, M.A., Huntley, R., Van Auken, K., Cherry, J.M., 2013. A guide to best practices for Gene Ontology (GO) manual annotation. Database (Oxford) 2013, bat054. https://doi.org/10.1093/database/bat054

Barragan, M., Good, M., Kolls, J.K., 2015. Regulation of Dendritic Cell Function by Vitamin D. Nutrients 7, 8127–8151. https://doi.org/10.3390/nu7095383

Benjamini, Y., Hochberg, Y., 1995. Controlling the False Discovery Rate: A Practical and Powerful Approach to Multiple Testing. Journal of the Royal Statistical Society. Series B (Methodological) 57, 289–300. https://doi.org/10.1111/j.2517-6161.1995.tb02031.x

Bertani, F.R., Mozetic, P., Fioramonti, M., Iuliani, M., Ribelli, G., Pantano, F., Santini, D., Tonini, G., Trombetta, M., Businaro, L., Selci, S., Rainer, A., 2017. Classification of M1/M2-polarized human macrophages by label-free hyperspectral reflectance confocal microscopy and multivariate analysis. Scientific Reports 7, 8965. https://doi.org/10.1038/s41598-017-08121-8

Blériot, C., Chakarov, S., Ginhoux, F., 2020. Determinants of Resident Tissue Macrophage Identity and Function. Immunity 52, 957–970. https://doi.org/10.1016/j.immuni.2020.05.014

Boulakirba, S., Pfeifer, A., Mhaidly, R., Obba, S., Goulard, M., Schmitt, T., Chaintreuil, P., Calleja, A., Furstoss, N., Orange, F., Lacas-Gervais, S., Boyer, L., Marchetti, S., Verhoeyen, E., Luciano, F., Robert, G., Auberger, P., Jacquel, A., 2018. IL-34 and CSF-1 display an equivalent macrophage differentiation ability but a different polarization potential. Sci Rep 8, 256. https://doi.org/10.1038/s41598-017-18433-4

Bray, N.L., Pimentel, H., Melsted, P., Pachter, L., 2016. Near-optimal probabilistic RNA-seq quantification. Nat Biotechnol 34, 525–527. https://doi.org/10.1038/nbt.3519

Browne, E., Kavanagh, S., Devery, S., 2022. The Cytotoxicity of Phorbol 12- Myristate 13-Acetate and Lipopolysaccharide on THP-1 Cells and an Optimized Differentiation

Protocol. Medical Sciences Forum 11, 5. https://doi.org/10.3390/BiTaP-12785

Bruckmeier, M., Kuehnl, A., Culmes, M., Pelisek, J., Eckstein, H.-H., 2012. Impact of oxLDL and LPS on C-type natriuretic peptide system is different between THP-1 cells and human peripheral blood monocytic cells. Cell Physiol Biochem 30, 199–209. https://doi.org/10.1159/000339044

Chang, S.N., Dey, D.K., Oh, S.T., Kong, W.H., Cho, K.H., Al-Olayan, E.M., Hwang, B.S., Kang, S.C., Park, J.G., 2020. Phorbol 12-Myristate 13-Acetate Induced Toxicity Study and the Role of Tangeretin in Abrogating HIF-1α-NF-κB Crosstalk In Vitro and In Vivo. Int J Mol Sci 21, 9261. https://doi.org/10.3390/ijms21239261

Chanput, W., Mes, J.J., Wichers, H.J., 2014. THP-1 cell line: An in vitro cell model for immune modulation approach. International Immunopharmacology 23, 37–45. https://doi.org/10.1016/j.intimp.2014.08.002

Chou, S.T., Khandros, E., Bailey, L.C., Nichols, K.E., Vakoc, C.R., Yao, Y., Huang, Z., Crispino, J.D., Hardison, R.C., Blobel, G.A., Weiss, M.J., 2009. Graded repression of PU.1/Sfpi1 gene transcription by GATA factors regulates hematopoietic cell fate. Blood 114, 983–994. https://doi.org/10.1182/blood-2009-03-207944

Compton, T., Kurt-Jones, E.A., Boehme, K.W., Belko, J., Latz, E., Golenbock, D.T., Finberg, R.W., 2003. Human Cytomegalovirus Activates Inflammatory Cytokine Responses via CD14 and Toll-Like Receptor 2. Journal of Virology 77, 4588–4596. https://doi.org/10.1128/JVI.77.8.4588-4596.2003

Dahl, R., Walsh, J.C., Lancki, D., Laslo, P., Iyer, S.R., Singh, H., Simon, M.C., 2003. Regulation of macrophage and neutrophil cell fates by the PU.1:C/EBPα ratio and granulocyte colony-stimulating factor. Nature Immunology 4, 1029–1036. https://doi.org/10.1038/ni973

Daigneault, M., Preston, J.A., Marriott, H.M., Whyte, M.K.B., Dockrell, D.H., 2010. The Identification of Markers of Macrophage Differentiation in PMA-Stimulated THP-1 Cells and Monocyte-Derived Macrophages. PLOS ONE 5, e8668. https://doi.org/10.1371/journal.pone.0008668

Das, H., Kumar, A., Lin, Z., Patino, W.D., Hwang, P.M., Feinberg, M.W., Majumder, P.K., Jain, M.K., 2006. Kruppel-like factor 2 (KLF2) regulates proinflammatory activation of monocytes. Proceedings of the National Academy of Sciences 103, 6653–6658. https://doi.org/10.1073/pnas.0508235103

Das, M., Lu, J., Joseph, M., Aggarwal, R., Kanji, S., McMichael, B.K., Lee, B.S., Agarwal, S., Ray-Chaudhury, A., Iwenofu, O.H., Kuppusamy, P., Pompili, V.J., Jain, M.K., Das, H.,

2012. Kruppel-like factor 2 (KLF2) regulates monocyte differentiation and functions in mBSA and IL-1β-induced arthritis. Curr Mol Med 12, 113–125. https://doi.org/10.2174/156652412798889090

Davies, L.C., Jenkins, S.J., Allen, J.E., Taylor, P.R., 2013. Tissue-resident macrophages. Nat Immunol 14, 986–995. https://doi.org/10.1038/ni.2705

De Kleer, I., Willems, F., Lambrecht, B., Goriely, S., 2014. Ontogeny of Myeloid Cells. Frontiers in Immunology 5. https://doi.org/10.3389/fimmu.2014.00423

DeLuca, H.F., 2014. History of the discovery of vitamin D and its active metabolites. Bonekey Rep 3, 479. https://doi.org/10.1038/bonekey.2013.213

Di Rosa, M., Malaguarnera, G., De Gregorio, C., Palumbo, M., Nunnari, G., Malaguarnera, L., 2012. Immuno-modulatory effects of vitamin D3 in human monocyte and macrophages. Cell Immunol 280, 36–43. https://doi.org/10.1016/j.cellimm.2012.10.009

Du, T., Zhou, Z.-G., You, S., Huang, G., Lin, J., Yang, L., Li, X., Zhou, W.-D., Chao, C., 2009. Modulation of monocyte hyperresponsiveness to TLR ligands by 1,25-dihydroxy-vitamin D3 from LADA and T2DM. Diabetes Res Clin Pract 83, 208–214. https://doi.org/10.1016/j.diabres.2008.09.046

Feinberg, M.W., Wara, A.K., Cao, Z., Lebedeva, M.A., Rosenbauer, F., Iwasaki, H., Hirai, H., Katz, J.P., Haspel, R.L., Gray, S., Akashi, K., Segre, J., Kaestner, K.H., Tenen, D.G., Jain, M.K., 2007. The Kruppel-like factor KLF4 is a critical regulator of monocyte differentiation. EMBO J 26, 4138–4148. https://doi.org/10.1038/sj.emboj.7601824

Ferrante, C.J., Pinhal-Enfield, G., Elson, G., Cronstein, B.N., Hasko, G., Outram, S., Leibovich, S.J., 2013. The adenosine-dependent angiogenic switch of macrophages to an M2-like phenotype is independent of interleukin-4 receptor alpha (IL-4Rα) signaling. Inflammation 36, 921–931. https://doi.org/10.1007/s10753-013-9621-3

Frankish, A., Diekhans, M., Ferreira, A.-M., Johnson, R., Jungreis, I., Loveland, J., Mudge, J.M., Sisu, C., Wright, J., Armstrong, J., Barnes, I., Berry, A., Bignell, A., Carbonell Sala, S., Chrast, J., Cunningham, F., Di Domenico, T., Donaldson, S., Fiddes, I.T., García Girón, C., Gonzalez, J.M., Grego, T., Hardy, M., Hourlier, T., Hunt, T., Izuogu, O.G., Lagarde, J., Martin, F.J., Martínez, L., Mohanan, S., Muir, P., Navarro, F.C.P., Parker, A., Pei, B., Pozo, F., Ruffier, M., Schmitt, B.M., Stapleton, E., Suner, M.-M., Sycheva, I., Uszczynska-Ratajczak, B., Xu, J., Yates, A., Zerbino, D., Zhang, Y., Aken, B., Choudhary, J.S., Gerstein, M., Guigó, R., Hubbard, T.J.P., Kellis, M., Paten, B., Reymond, A., Tress, M.L., Flicek, P., 2019. GENCODE reference annotation for the

human and mouse genomes. Nucleic Acids Res 47, D766–D773. https://doi.org/10.1093/nar/gky955

Friedman, A.D., 2002. Transcriptional regulation of myelopoiesis. Int J Hematol 75, 466–472. https://doi.org/10.1007/BF02982108

Gažová, I., Lefevre, L., Bush, S.J., Clohisey, S., Arner, E., de Hoon, M., Severin, J., van Duin, L., Andersson, R., Lengeling, A., Hume, D.A., Summers, K.M., 2020. The Transcriptional Network That Controls Growth Arrest and Macrophage Differentiation in the Human Myeloid Leukemia Cell Line THP-1. Frontiers in Cell and Developmental Biology 8, 498. https://doi.org/10.3389/fcell.2020.00498

Gemelli, C., Montanari, M., Tenedini, E., Zanocco Marani, T., Vignudelli, T., Siena, M., Zini, R., Salati, S., Tagliafico, E., Manfredini, R., Grande, A., Ferrari, S., 2006. Virally mediated MafB transduction induces the monocyte commitment of human CD34+ hematopoietic stem/progenitor cells. Cell Death Differ 13, 1686–1696. https://doi.org/10.1038/sj.cdd.4401860

Girardin, S.E., Boneca, I.G., Carneiro, L.A.M., Antignac, A., Jéhanno, M., Viala, J., Tedin, K., Taha, M.-K., Labigne, A., Zäthringer, U., Coyle, A.J., DiStefano, P.S., Bertin, J., Sansonetti, P.J., Philpott, D.J., 2003. Nod1 Detects a Unique Muropeptide from Gram-Negative Bacterial Peptidoglycan. Science 300, 1584–1587. https://doi.org/10.1126/science.1084677

González-Sancho, J.M., Alvarez-Dolado, M., Muñoz, A., 1998. 1,25-Dihydroxyvitamin D3 inhibits tenascin-C expression in mammary epithelial cells. FEBS Letters 426, 225–228. https://doi.org/10.1016/S0014-5793(98)00348-2

Grinberg, S., Hasko, G., Wu, D., Leibovich, S.J., 2009. Suppression of PLCbeta2 by endotoxin plays a role in the adenosine A(2A) receptor-mediated switch of macrophages from an inflammatory to an angiogenic phenotype. Am J Pathol 175, 2439–2453. https://doi.org/10.2353/ajpath.2009.090290

Henning, L.N., Azad, A.K., Parsa, K.V.L., Crowther, J.E., Tridandapani, S., Schlesinger, L.S., 2008. Pulmonary Surfactant Protein A Regulates TLR Expression and Activity in Human Macrophages1. J Immunology 180, 7847–7858. https://doi.org/10.4049/jimmunol.180.12.7847

Hettinger, J., Richards, D.M., Hansson, J., Barra, M.M., Joschko, A.-C., Krijgsveld, J., Feuerer, M., 2013. Origin of monocytes and macrophages in a committed progenitor. Nat Immunol 14, 821–830. https://doi.org/10.1038/ni.2638

Hjort, M.R., Brenyo, A.J., Finkelstein, J.N., Frampton, M.W., LoMonaco, M.B., Stewart, J.C.,

Johnston, C.J., D'Angio, C.T., 2003. Alveolar epithelial cell-macrophage interactions affect oxygen-stimulated interleukin-8 release. Inflammation 27, 137–145. https://doi.org/10.1023/a:1023817811850

Holick, M.F., 2009. Vitamin D Status: Measurement, Interpretation, and Clinical Application. Ann Epidemiol 19, 73–78. https://doi.org/10.1016/j.annepidem.2007.12.001

Hristodorov, D., Mladenov, R., von Felbert, V., Huhn, M., Fischer, R., Barth, S., Thepen, T., 2015. Targeting CD64 mediates elimination of M1 but not M2 macrophages in vitro and in cutaneous inflammation in mice and patient biopsies. mAbs 7, 853–862. https://doi.org/10.1080/19420862.2015.1066950

Huang, D.W., Sherman, B.T., Lempicki, R.A., 2009. Bioinformatics enrichment tools: paths toward the comprehensive functional analysis of large gene lists. Nucleic Acids Res 37, 1–13. https://doi.org/10.1093/nar/gkn923

Huang, S., Zhu, B., Cheon, I.S., Goplen, N.P., Jiang, L., Zhang, R., Peebles, R.S., Mack, M., Kaplan, M.H., Limper, A.H., Sun, J., 2019. PPAR-γ in Macrophages Limits Pulmonary Inflammation and Promotes Host Recovery following Respiratory Viral Infection. J Virol 93, e00030-19. https://doi.org/10.1128/JVI.00030-19

Janeway, C.A., Medzhitov, R., 2002. Innate Immune Recognition. Annual Review of Immunology 20, 197–216. https://doi.org/10.1146/annurev.immunol.20.083001.084359

Jayaraman, P., Sada-Ovalle, I., Beladi, S., Anderson, A.C., Dardalhon, V., Hotta, C., Kuchroo, V.K., Behar, S.M., 2010. Tim3 binding to galectin-9 stimulates antimicrobial immunity. J Exp Med 207, 2343–2354. https://doi.org/10.1084/jem.20100687

Jayaraman, P., Sada-Ovalle, I., Nishimura, T., Anderson, A.C., Kuchroo, V.K., Remold, H.G., Behar, S.M., 2013. IL-1β Promotes Antimicrobial Immunity in Macrophages by Regulating TNFR Signaling and caspase-3 activation. J Immunol 190, 4196–4204. https://doi.org/10.4049/jimmunol.1202688

Jenkins, S.J., Ruckerl, D., Thomas, G.D., Hewitson, J.P., Duncan, S., Brombacher, F., Maizels, R.M., Hume, D.A., Allen, J.E., 2013. IL-4 directly signals tissue-resident macrophages to proliferate beyond homeostatic levels controlled by CSF-1. J Expl Med 210, 2477–2491. https://doi.org/10.1084/jem.20121999

Kanehisa, M., Goto, S., Furumichi, M., Tanabe, M., Hirakawa, M., 2010. KEGG for representation and analysis of molecular networks involving diseases and drugs. Nucleic Acids Res. 38, D355-360. https://doi.org/10.1093/nar/gkp896

Karp, P.D., Midford, P.E., Caspi, R., Khodursky, A., 2021. Pathway size matters: the influence

of pathway granularity on over-representation (enrichment analysis) statistics. BMC Genom 22, 191. https://doi.org/10.1186/s12864-021-07502-8

Kawamura, S., Onai, N., Miya, F., Sato, T., Tsunoda, T., Kurabayashi, K., Yotsumoto, S., Kuroda, S., Takenaka, K., Akashi, K., Ohteki, T., 2017. Identification of a Human Clonogenic Progenitor with Strict Monocyte Differentiation Potential: A Counterpart of Mouse cMoPs. Immunity 46, 835-848.e4. https://doi.org/10.1016/j.immuni.2017.04.019

Koeffler, H.P., Amatruda, T., Ikekawa, N., Kobayashi, Y., DeLuca, H.F., 1984. Induction of macrophage differentiation of human normal and leukemic myeloid stem cells by 1,25-dihydroxyvitamin D3 and its fluorinated analogues. Cancer Res 44, 5624–5628.

Kohro, T., Tanaka, T., Murakami, T., Wada, Y., Aburatani, H., Hamakubo, T., Kodama, T., 2004. A comparison of differences in the gene expression profiles of phorbol 12-myristate 13-acetate differentiated THP-1 cells and human monocyte-derived macrophage. J. Atheroscler. Thromb. 11, 88–97. https://doi.org/10.5551/jat.11.88

Kramer, P.R., Wray, S., 2002. 17-Beta-estradiol regulates expression of genes that function in macrophage activation and cholesterol homeostasis. J Steroid Biochem Mol Biol 81, 203–216. https://doi.org/10.1016/s0960-0760(02)00065-1

Kurotaki, D., Osato, N., Nishiyama, A., Yamamoto, M., Ban, T., Sato, H., Nakabayashi, J., Umehara, M., Miyake, N., Matsumoto, N., Nakazawa, M., Ozato, K., Tamura, T., 2013. Essential role of the IRF8-KLF4 transcription factor cascade in murine monocyte differentiation. Blood 121, 1839–1849. https://doi.org/10.1182/blood-2012-06-437863

Lee, J.Y., Hong, S.-H., 2019. Hematopoietic Stem Cells and Their Roles in Tissue Regeneration. Int J Stem Cells 13, 1–12. https://doi.org/10.15283/ijsc19127

Levin, J.Z., Yassour, M., Adiconis, X., Nusbaum, C., Thompson, D.A., Friedman, N., Gnirke, A., Regev, A., 2010. Comprehensive comparative analysis of strand-specific RNA sequencing methods. Nat Methods 7, 709–715. https://doi.org/10.1038/nmeth.1491

Lewis, M.R., Lewis, W.H., 1925. The transformation of white blood cells: into clasmatocytes (macrophages), epithelioid cells, and giant cells. Journal of the American Medical Association 84, 798–799. https://doi.org/10.1001/jama.1925.02660370008002

Lips, P., 2006. Vitamin D physiology. Progress in Biophysics and Molecular Biology, UV exposure guidance: A balanced approach between health risks and health benefits of UV and Vitamin D. Proceedings of an International Workshop, International Commission on Non-ionizing Radiation Protection, Munich, Germany, 17-18 October, 2005 92, 4–8. https://doi.org/10.1016/j.pbiomolbio.2006.02.016

Liu, H., Lorenzini, P.A., Zhang, F., Xu, S., Wong, M.S.M., Zheng, J., Roca, X., 2018. Alternative splicing analysis in human monocytes and macrophages reveals MBNL1 as major regulator. Nucleic Acids Res 46, 6069–6086. https://doi.org/10.1093/nar/gky401

Liu, P.T., Stenger, S., Li, H., Wenzel, L., Tan, B.H., Krutzik, S.R., Ochoa, M.T., Schauber, J., Wu, K., Meinken, C., Kamen, D.L., Wagner, M., Bals, R., Steinmeyer, A., Zügel, U., Gallo, R.L., Eisenberg, D., Hewison, M., Hollis, B.W., Adams, J.S., Bloom, B.R., Modlin, R.L., 2006. Toll-Like Receptor Triggering of a Vitamin D-Mediated Human Antimicrobial Response. Science 311, 1770–1773. https://doi.org/10.1126/science.1123933

Liu, P.T., Stenger, S., Tang, D.H., Modlin, R.L., 2007. Cutting edge: vitamin D-mediated human antimicrobial activity against Mycobacterium tuberculosis is dependent on the induction of cathelicidin. J Immunol 179, 2060–2063. https://doi.org/10.4049/jimmunol.179.4.2060

Liu, Y., Shi, L., Qiu, W., Shi, Y., 2022. Ferulic acid exhibits anti-inflammatory effects by inducing autophagy and blocking NLRP3 inflammasome activation. Mol Cell Toxicol 18, 509–519. https://doi.org/10.1007/s13273-021-00219-5

Liu, Z.-Z., Han, Z.-D., Liang, Y.-K., Chen, J.-X., Wan, S., Zhuo, Y.-J., Cai, Z.-D., Deng, Y.-L., Lin, Z.-Y., Mo, R.-J., He, H.-C., Zhong, W.-D., 2019. TRIB1 induces macrophages to M2 phenotype by inhibiting IKB-zeta in prostate cancer. Cellular Signalling 59, 152–162. https://doi.org/10.1016/j.cellsig.2019.03.017

Love, M.I., Hogenesch, J.B., Irizarry, R.A., 2016. Modeling of RNA-seq fragment sequence bias reduces systematic errors in transcript abundance estimation. Nat Biotechnol 34, 1287–1291. https://doi.org/10.1038/nbt.3682

Love, M.I., Huber, W., Anders, S., 2014. Moderated estimation of fold change and dispersion for RNA-seq data with DESeq2. Genome Biol 15. https://doi.org/10.1186/s13059-014-0550-8

Love, M.I., Soneson, C., Hickey, P.F., Johnson, L.K., Pierce, N.T., Shepherd, L., Morgan, M., Patro, R., 2019. Tximeta: reference sequence checksums for provenance identification in RNA-seq. bioRxiv 777888. https://doi.org/10.1101/777888

Lund, M.E., To, J., O'Brien, B.A., Donnelly, S., 2016. The choice of phorbol 12-myristate 13-acetate differentiation protocol influences the response of THP-1 macrophages to a pro-inflammatory stimulus. Journal of Immunological Methods 430, 64–70. https://doi.org/10.1016/j.jim.2016.01.012

Luo, W., Brouwer, C., 2013. Pathview: an R/Bioconductor package for pathway-based data

integration and visualization. Bioinformatics 29, 1830–1831. https://doi.org/10.1093/bioinformatics/btt285

Mantovani, A., Sica, A., Sozzani, S., Allavena, P., Vecchi, A., Locati, M., 2004. The chemokine system in diverse forms of macrophage activation and polarization. Trends in Immunology 25, 677–686. https://doi.org/10.1016/j.it.2004.09.015

Martinez, F.O., Gordon, S., Locati, M., Mantovani, A., 2006. Transcriptional Profiling of the Human Monocyte-to-Macrophage Differentiation and Polarization: New Molecules and Patterns of Gene Expression. The Journal of Immunology 177, 7303–7311. https://doi.org/10.4049/jimmunol.177.10.7303

Martinon, F., Tschopp, J., 2004. Inflammatory Caspases: Linking an Intracellular Innate Immune System to Autoinflammatory Diseases. Cell 117, 561–574. https://doi.org/10.1016/j.cell.2004.05.004

Matilainen, J.M., Husso, T., Toropainen, S., Seuter, S., Turunen, M.P., Gynther, P., Ylä-Herttuala, S., Carlberg, C., Väisänen, S., 2010. Primary effect of 1α,25(OH)$_2$D$_3$ on IL-10 expression in monocytes is short-term down-regulation. Biochim Biophys Acta 1803, 1276–1286. https://doi.org/10.1016/j.bbamcr.2010.07.009

Medrano, M., Carrillo-Cruz, E., Montero, I., Perez-Simon, J.A., 2018. Vitamin D: Effect on Haematopoiesis and Immune System and Clinical Applications. International Journal of Molecular Sciences 19, 2663. https://doi.org/10.3390/ijms19092663

Medzhitov, R., Preston-Hurlburt, P., Janeway, C.A., 1997. A human homologue of the Drosophila Toll protein signals activation of adaptive immunity. Nature 388, 394–397. https://doi.org/10.1038/41131

Meraro, D., Hashmueli, S., Koren, B., Azriel, A., Oumard, A., Kirchhoff, S., Hauser, H., Nagulapalli, S., Atchison, M.L., Levi, B.Z., 1999. Protein-protein and DNA-protein interactions affect the activity of lymphoid-specific IFN regulatory factors. J Immunol 163, 6468–6478.

Metchnikoff, 1883. Untersuchungen über die mesodermalen Phagocyten einiger Wirbeltiere. Biol Zentralbl 560–565.

Metschnikoff, E., 1891. Lecture on Phagocytosis and Immunity. Br Med J 1, 213–217. https://doi.org/10.1136/bmj.1.1570.213

Misharin, A.V., Morales-Nebreda, L., Mutlu, G.M., Budinger, G.R.S., Perlman, H., 2013. Flow Cytometric Analysis of Macrophages and Dendritic Cell Subsets in the Mouse Lung. Am J Respir Cell Mol Biol 49, 503–510. https://doi.org/10.1165/rcmb.2013-0086MA

Mosser, D.M., 2003. The many faces of macrophage activation. J Leukoc Biol 73, 209–212.

https://doi.org/10.1189/jlb.0602325

Mosser, D.M., Edwards, J.P., 2008. Exploring the full spectrum of macrophage activation. Nat Rev Immunol 8, 958–969. https://doi.org/10.1038/nri2448

Mosser, D.M., Hamidzadeh, K., Goncalves, R., 2020. Macrophages and the maintenance of homeostasis. Cellular & Molecular Immunology 1–9. https://doi.org/10.1038/s41423-020-00541-3

Munker, R., Norman, A., Koeffler, H.P., 1986. Vitamin D compounds. Effect on clonal proliferation and differentiation of human myeloid cells. J Clin Invest 78, 424–430. https://doi.org/10.1172/JCI112593

Murphy, K., Weaver, C., 2016. Janeway's Immunobiology, 9th edition. ed. Garland Science, New York, NY.

Murray, P.J., Wynn, T.A., 2011. Protective and pathogenic functions of macrophage subsets. Nat Rev Immunol 11, 723–737. https://doi.org/10.1038/nri3073

Naik, S.H., Metcalf, D., van Nieuwenhuijze, A., Wicks, I., Wu, L., O'Keeffe, M., Shortman, K., 2006. Intrasplenic steady-state dendritic cell precursors that are distinct from monocytes. Nat Immunol 7, 663–671. https://doi.org/10.1038/ni1340

Novershtern, N., Subramanian, A., Lawton, L.N., Mak, R.H., Haining, W.N., McConkey, M.E., Habib, N., Yosef, N., Chang, C.Y., Shay, T., Frampton, G.M., Drake, A.C.B., Leskov, I., Nilsson, B., Preffer, F., Dombkowski, D., Evans, J.W., Liefeld, T., Smutko, J.S., Chen, J., Friedman, N., Young, R.A., Golub, T.R., Regev, A., Ebert, B.L., 2011. Densely Interconnected Transcriptional Circuits Control Cell States in Human Hematopoiesis. Cell 144, 296–309. https://doi.org/10.1016/j.cell.2011.01.004

Nurminen, V., Neme, A., Seuter, S., Carlberg, C., 2019. Modulation of vitamin D signaling by the pioneer factor CEBPA. Biochim Biophys Acta Gene Regul Mech 1862, 96–106. https://doi.org/10.1016/j.bbagrm.2018.12.004

Nutt, S.L., Metcalf, D., D'Amico, A., Polli, M., Wu, L., 2005. Dynamic regulation of PU.1 expression in multipotent hematopoietic progenitors. J Exp Med 201, 221–231. https://doi.org/10.1084/jem.20041535

Oshlack, A., Robinson, M.D., Young, M.D., 2010. From RNA-seq reads to differential expression results. Genome Biol 11, 220. https://doi.org/10.1186/gb-2010-11-12-220

Park, E.K., Jung, H.S., Yang, H.I., Yoo, M.C., Kim, C., Kim, K.S., 2007. Optimized THP-1 differentiation is required for the detection of responses to weak stimuli. Inflamm. res. 56, 45–50. https://doi.org/10.1007/s00011-007-6115-5

Passlick, B., Flieger, D., Ziegler-Heitbrock, H.W., 1989. Identification and characterization of

a novel monocyte subpopulation in human peripheral blood. Blood 74, 2527–2534.

Patro, R., Duggal, G., Love, M.I., Irizarry, R.A., Kingsford, C., 2017. Salmon: fast and bias-aware quantification of transcript expression using dual-phase inference. Nat Methods 14, 417–419. https://doi.org/10.1038/nmeth.4197

Peters, W., Scott, H.M., Chambers, H.F., Flynn, J.L., Charo, I.F., Ernst, J.D., 2001. Chemokine receptor 2 serves an early and essential role in resistance to Mycobacterium tuberculosis. Proc Natl Acad Sci U S A 98, 7958–7963. https://doi.org/10.1073/pnas.131207398

Pietras, E.M., Reynaud, D., Kang, Y.-A., Carlin, D., Calero-Nieto, F.J., Leavitt, A.D., Stuart, J.M., Göttgens, B., Passegué, E., 2015. Functionally Distinct Subsets of Lineage-Biased Multipotent Progenitors Control Blood Production in Normal and Regenerative Conditions. Cell Stem Cell 17, 35–46. https://doi.org/10.1016/j.stem.2015.05.003

Pixley, F.J., Stanley, E.R., 2004. CSF-1 regulation of the wandering macrophage: complexity in action. Trends in Cell Biology 14, 628–638. https://doi.org/10.1016/j.tcb.2004.09.016

Pramanik, R., Asplin, J.R., Lindeman, C., Favus, M.J., Bai, S., Coe, F.L., 2004. Lipopolysaccharide negatively modulates vitamin D action by down-regulating expression of vitamin D-induced VDR in human monocytic THP-1 cells. Cell Immunol 232, 137–143. https://doi.org/10.1016/j.cellimm.2005.03.004

Qin, Z., 2012. The use of THP-1 cells as a model for mimicking the function and regulation of monocytes and macrophages in the vasculature. Atherosclerosis 221, 2–11. https://doi.org/10.1016/j.atherosclerosis.2011.09.003

Radomska, H.S., Huettner, C.S., Zhang, P., Cheng, T., Scadden, D.T., Tenen, D.G., 1998. CCAAT/enhancer binding protein alpha is a regulatory switch sufficient for induction of granulocytic development from bipotential myeloid progenitors. Mol Cell Biol 18, 4301–4314. https://doi.org/10.1128/MCB.18.7.4301

Reddy, V.A., Iwama, A., Iotzova, G., Schulz, M., Elsasser, A., Vangala, R.K., Tenen, D.G., Hiddemann, W., Behre, G., 2002. Granulocyte inducer C/EBPalpha inactivates the myeloid master regulator PU.1: possible role in lineage commitment decisions. Blood 100, 483–490. https://doi.org/10.1182/blood.v100.2.483

Risso, D., Schwartz, K., Sherlock, G., Dudoit, S., 2011. GC-Content Normalization for RNA-Seq Data. BMC Bioinformatics 12, 480. https://doi.org/10.1186/1471-2105-12-480

Roberts, A., Trapnell, C., Donaghey, J., Rinn, J.L., Pachter, L., 2011. Improving RNA-Seq expression estimates by correcting for fragment bias. Genome Biology 12, R22.

https://doi.org/10.1186/gb-2011-12-3-r22

Roberts, M.E., Barvalia, M., Silva, J.A.F.D., Cederberg, R.A., Chu, W., Wong, A., Tai, D.C., Chen, S., Matos, I., Priatel, J.J., Cullis, P.R., Harder, K.W., 2020. Deep Phenotyping by Mass Cytometry and Single-Cell RNA-Sequencing Reveals LYN-Regulated Signaling Profiles Underlying Monocyte Subset Heterogeneity and Lifespan. Circulation Research 126, e61–e79. https://doi.org/10.1161/CIRCRESAHA.119.315708

Röthlisberger, B., Heizmann, M., Bargetzi, M.J., Huber, A.R., 2007. TRIB1 overexpression in acute myeloid leukemia. Cancer Genetics and Cytogenetics 176, 58–60. https://doi.org/10.1016/j.cancergencyto.2007.03.003

Rovera, G., Santoli, D., Damsky, C., 1979. Human promyelocytic leukemia cells in culture differentiate into macrophage-like cells when treated with a phorbol diester. Proc. Natl. Acad. Sci. U.S.A. 76, 2779–2783. https://doi.org/10.1073/pnas.76.6.2779

Sadeghi, K., Wessner, B., Laggner, U., Ploder, M., Tamandl, D., Friedl, J., Zügel, U., Steinmeyer, A., Pollak, A., Roth, E., Boltz-Nitulescu, G., Spittler, A., 2006. Vitamin D3 down-regulates monocyte TLR expression and triggers hyporesponsiveness to pathogen-associated molecular patterns. European Journal of Immunology 36, 361–370. https://doi.org/10.1002/eji.200425995

Saeed, S., Quintin, J., Kerstens, H.H.D., Rao, N.A., Aghajanirefah, A., Matarese, F., Cheng, S.-C., Ratter, J., Berentsen, K., van der Ent, M.A., Sharifi, N., Janssen-Megens, E.M., Huurne, M.T., Mandoli, A., van Schaik, T., Ng, A., Burden, F., Downes, K., Frontini, M., Kumar, V., Giamarellos-Bourboulis, E.J., Ouwehand, W.H., van der Meer, J.W.M., Joosten, L.A.B., Wijmenga, C., Martens, J.H.A., Xavier, R.J., Logie, C., Netea, M.G., Stunnenberg, H.G., 2014. Epigenetic programming during monocyte to macrophage differentiation and trained innate immunity. Science 345, 1251086. https://doi.org/10.1126/science.1251086

Salazar-Mather, T.P., Orange, J.S., Biron, C.A., 1998. Early Murine Cytomegalovirus (MCMV) Infection Induces Liver Natural Killer (NK) Cell Inflammation and Protection Through Macrophage Inflammatory Protein 1α (MIP-1α)–dependent Pathways. J Exp Med 187, 1–14. https://doi.org/10.1084/jem.187.1.1

Sarantopoulou, D., Brooks, T.G., Nayak, S., Mrčela, A., Lahens, N.F., Grant, G.R., 2021. Comparative evaluation of full-length isoform quantification from RNA-Seq. BMC Bioinform 22, 266. https://doi.org/10.1186/s12859-021-04198-1

Sarkar, H., Zakeri, M., Malik, L., Patro, R., 2017. Towards selective-alignment: Bridging the

accuracy gap between alignment-based and alignment-free transcript quantification. bioRxiv 138800. https://doi.org/10.1101/138800

Satoh, T., Kidoya, H., Naito, H., Yamamoto, M., Takemura, N., Nakagawa, K., Yoshioka, Y., Morii, E., Takakura, N., Takeuchi, O., Akira, S., 2013. Critical role of Trib1 in differentiation of tissue-resident M2-like macrophages. Nature 495, 524–528. https://doi.org/10.1038/nature11930

Schildberger, A., Rossmanith, E., Eichhorn, T., Strassl, K., Weber, V., 2013. Monocytes, peripheral blood mononuclear cells, and THP-1 cells exhibit different cytokine expression patterns following stimulation with lipopolysaccharide. Mediators Inflamm 2013, 697972. https://doi.org/10.1155/2013/697972

Schroecksnadel, S., Jenny, M., Fuchs, D., 2011. Myelomonocytic THP-1 cells for in vitro testing of immunomodulatory properties of nanoparticles. J Biomed Nanotechnol 7, 209–210. https://doi.org/10.1166/jbn.2011.1272

Schwende, H., Fitzke, E., Ambs, P., Dieter, P., 1996. Differences in the state of differentiation of THP-1 cells induced by phorbol ester and 1,25-dihydroxyvitamin D3. J Leukoc Biol 59, 555–561.

Serbina, N.V., Kuziel, W., Flavell, R., Akira, S., Rollins, B., Pamer, E.G., 2003. Sequential MyD88-independent and -dependent activation of innate immune responses to intracellular bacterial infection. Immunity 19, 891–901. https://doi.org/10.1016/s1074-7613(03)00330-3

Seuter, S., Neme, A., Carlberg, C., 2017. Epigenomic PU.1-VDR crosstalk modulates vitamin D signaling. Biochim Biophys Acta Gene Regul Mech 1860, 405–415. https://doi.org/10.1016/j.bbagrm.2017.02.005

Seuter, S., Pehkonen, P., Heikkinen, S., Carlberg, C., 2013. Dynamics of 1α,25-dihydroxyvitamin D3-dependent chromatin accessibility of early vitamin D receptor target genes. Biochimica et Biophysica Acta (BBA) - Gene Regulatory Mechanisms 1829, 1266–1275. https://doi.org/10.1016/j.bbagrm.2013.10.003

Sheu, K.M., Hoffmann, A., 2022. Functional Hallmarks of Healthy Macrophage Responses: Their Regulatory Basis and Disease Relevance. Annu Rev Immunol 40, 295–321. https://doi.org/10.1146/annurev-immunol-101320-031555

Shiratori, H., Feinweber, C., Luckhardt, S., Linke, B., Resch, E., Geisslinger, G., Weigert, A., Parnham, M.J., 2017. THP-1 and human peripheral blood mononuclear cell-derived macrophages differ in their capacity to polarize in vitro. Molecular Immunology 88, 58–68. https://doi.org/10.1016/j.molimm.2017.05.027

Sieweke, M.H., Allen, J.E., 2013. Beyond Stem Cells: Self-Renewal of Differentiated Macrophages. Science 342, 1242974. https://doi.org/10.1126/science.1242974

Sieweke, M.H., Tekotte, H., Frampton, J., Graf, T., 1996. MafB Is an Interaction Partner and Repressor of Ets-1 That Inhibits Erythroid Differentiation. Cell 85, 49–60. https://doi.org/10.1016/S0092-8674(00)81081-8

Sims, D., Sudbery, I., Ilott, N.E., Heger, A., Ponting, C.P., 2014. Sequencing depth and coverage: key considerations in genomic analyses. Nat Rev Genet 15, 121–132. https://doi.org/10.1038/nrg3642

Soneson, C., Love, M.I., Robinson, M.D., 2016. Differential analyses for RNA-seq: transcript-level estimates improve gene-level inferences. F1000Res 4, 1521. https://doi.org/10.12688/f1000research.7563.2

Srivastava, A., Malik, L., Sarkar, H., Zakeri, M., Almodaresi, F., Soneson, C., Love, M.I., Kingsford, C., Patro, R., 2020. Alignment and mapping methodology influence transcript abundance estimation. Genome Biol 21, 239. https://doi.org/10.1186/s13059-020-02151-8

Srivastava, A., Sarkar, H., Gupta, N., Patro, R., 2016. RapMap: a rapid, sensitive and accurate tool for mapping RNA-seq reads to transcriptomes. Bioinformatics 32, i192–i200. https://doi.org/10.1093/bioinformatics/btw277

Stark, R., Grzelak, M., Hadfield, J., 2019. RNA sequencing: the teenage years. Nat Rev Genet 20, 631–656. https://doi.org/10.1038/s41576-019-0150-2

Starr, T., Bauler, T.J., Malik-Kale, P., Steele-Mortimer, O., 2018. The phorbol 12-myristate-13-acetate differentiation protocol is critical to the interaction of THP-1 macrophages with Salmonella Typhimurium. PLoS One 13, e0193601. https://doi.org/10.1371/journal.pone.0193601

Steinbach, F., Thiele, B., 1994. Phenotypic investigation of mononuclear phagocytes by flow cytometry. Journal of Immunological Methods 174, 109–122. https://doi.org/10.1016/0022-1759(94)90015-9

Steingrimsson, E., Tessarollo, L., Pathak, B., Hou, L., Arnheiter, H., Copeland, N.G., Jenkins, N.A., 2002. Mitf and Tfe3, two members of the Mitf-Tfe family of bHLH-Zip transcription factors, have important but functionally redundant roles in osteoclast development. Proc Natl Acad Sci U S A 99, 4477–4482. https://doi.org/10.1073/pnas.072071099

Tamura, T., Thotakura, P., Tanaka, T.S., Ko, M.S.H., Ozato, K., 2005. Identification of target genes and a unique cis element regulated by IRF-8 in developing macrophages. Blood

106, 1938–1947. https://doi.org/10.1182/blood-2005-01-0080

Tanaka, H., Abe, E., Miyaura, C., Shiina, Y., Suda, T., 1983. 1 alpha,25-dihydroxyvitamin D3 induces differentiation of human promyelocytic leukemia cells (HL-60) into monocyte-macrophages, but not into granulocytes. Biochem Biophys Res Commun 117, 86–92. https://doi.org/10.1016/0006-291x(83)91544-9

Taylor, S.E., Gafur, M.A., Choudhury, A.K., Evans, F.J., 1981. Sapintoxin A, a new biologically active nitrogen containing phorbol ester. Experientia 37, 681–682. https://doi.org/10.1007/BF01967918

Tedesco, S., De Majo, F., Kim, J., Trenti, A., Trevisi, L., Fadini, G.P., Bolego, C., Zandstra, P.W., Cignarella, A., Vitiello, L., 2018. Convenience versus Biological Significance: Are PMA-Differentiated THP-1 Cells a Reliable Substitute for Blood-Derived Macrophages When Studying in Vitro Polarization? Front Pharmacol 9, 71. https://doi.org/10.3389/fphar.2018.00071

Thomas, G.D., Hamers, A.A., Nakao, C., Marcovecchio, P., Taylor, A.M., McSkimming, C., Nguyen, A.T., McNamara, C.A., Hedrick, C.C., 2017. Human blood monocyte subsets: a new gating strategy defined using cell surface markers identified by mass cytometry. Arterioscler Thromb Vasc Biol 37, 1548–1558. https://doi.org/10.1161/ATVBAHA.117.309145

Tsuchiya, S., Yamabe, M., Yamaguchi, Y., Kobayashi, Y., Konno, T., Tada, K., 1980. Establishment and characterization of a human acute monocytic leukemia cell line (THP-1). Int. J. Cancer 26, 171–176. https://doi.org/10.1002/ijc.2910260208

Tsujimura, H., Nagamura-Inoue, T., Tamura, T., Ozato, K., 2002. IFN consensus sequence binding protein/IFN regulatory factor-8 guides bone marrow progenitor cells toward the macrophage lineage. J Immunol 169, 1261–1269. https://doi.org/10.4049/jimmunol.169.3.1261

Tulk, S.E., Liao, K.-C., Muruve, D.A., Li, Y., Beck, P.L., MacDonald, J.A., 2015. Vitamin D_3 metabolites enhance the NLRP3-dependent secretion of IL-1β from human THP-1 monocytic cells. J Cell Biochem 116, 711–720. https://doi.org/10.1002/jcb.24985

Valdés López, J.F., Urcuqui-Inchima, S., 2018. Synergism between phorbol-12-myristate-13-acetate and vitamin D3 in the differentiation of U937 cells to monocytes and macrophages. Morphologie 102, 205–218. https://doi.org/10.1016/j.morpho.2018.06.001

van Furth, R., Sluiter, W., 1986. Distribution of blood monocytes between a marginating and a circulating pool. J Exp Med 163, 474–479. https://doi.org/10.1084/jem.163.2.474

Wallner, S., Schröder, C., Leitão, E., Berulava, T., Haak, C., Beißer, D., Rahmann, S., Richter, A.S., Manke, T., Bönisch, U., Arrigoni, L., Fröhler, S., Klironomos, F., Chen, W., Rajewsky, N., Müller, F., Ebert, P., Lengauer, T., Barann, M., Rosenstiel, P., Gasparoni, G., Nordström, K., Walter, J., Brors, B., Zipprich, G., Felder, B., Klein-Hitpass, L., Attenberger, C., Schmitz, G., Horsthemke, B., 2016. Epigenetic dynamics of monocyte-to-macrophage differentiation. Epigenetics & Chromatin 9, 33. https://doi.org/10.1186/s13072-016-0079-z

Walsh, J.C., DeKoter, R.P., Lee, H.J., Smith, E.D., Lancki, D.W., Gurish, M.F., Friend, D.S., Stevens, R.L., Anastasi, J., Singh, H., 2002. Cooperative and antagonistic interplay between PU.1 and GATA-2 in the specification of myeloid cell fates. Immunity 17, 665–676. https://doi.org/10.1016/s1074-7613(02)00452-1

Wang, Y.-C., Hsieh, C.-C., Kuo, H.-F., Tsai, M.-K., Yang, S.-N., Kuo, C.-H., Lee, M.-S., Hung, C.-H., 2014. Effect of Vitamin D3 on Monocyte Chemoattractant Protein 1 Production in Monocytes and Macrophages. Acta Cardiol Sin 30, 144–150.

Warwick, T., Schulz, M., Günther, S., Gilsbach, R., Neme, A., Brandes, R., Seuter, S., 2021. A hierarchical regulatory network analysis of the vitamin D induced transcriptome reveals novel regulators and complete VDR dependency in monocytes. Scientific Reports 11, 6518. https://doi.org/10.1038/s41598-021-86032-5

Wieder, C., Frainay, C., Poupin, N., Rodríguez-Mier, P., Vinson, F., Cooke, J., Lai, R.P., Bundy, J.G., Jourdan, F., Ebbels, T., 2021. Pathway analysis in metabolomics: Recommendations for the use of over-representation analysis. PLOS Comput Biol 17, e1009105. https://doi.org/10.1371/journal.pcbi.1009105

Wu, C., Li, F., Zhang, X., Xu, W., Wang, Y., Yao, Y., Han, Z., Xia, D., 2022. (-)-Epicatechin Ameliorates Monosodium Urate-Induced Acute Gouty Arthritis Through Inhibiting NLRP3 Inflammasome and the NF-κB Signaling Pathway. Front Pharmacol 13, 799552. https://doi.org/10.3389/fphar.2022.799552

Wu, T., Hu, E., Xu, S., Chen, M., Guo, P., Dai, Z., Feng, T., Zhou, L., Tang, W., Zhan, L., Fu, X., Liu, S., Bo, X., Yu, G., 2021. clusterProfiler 4.0: A universal enrichment tool for interpreting omics data. The Innovation 2, 100141. https://doi.org/10.1016/j.xinn.2021.100141

Wu, Y., Lin, X., Song, F., Xue, D., Wang, Y., 2022. Vitamin D3 promotes autophagy in THP-1 cells infected with Mycobacterium tuberculosis. Exp Ther Med 23, 240. https://doi.org/10.3892/etm.2022.11165

Wynn, T.A., Chawla, A., Pollard, J.W., 2013. Macrophage biology in development,

homeostasis and disease. Nature 496, 445–455. https://doi.org/10.1038/nature12034

Yalcin, F., Dzaye, O., Xia, S., 2020. Tenascin-C Function in Glioma: Immunomodulation and Beyond, in: Birbrair, A. (Ed.), Tumor Microenvironment : Extracellular Matrix Components – Part B, Advances in Experimental Medicine and Biology. Springer International Publishing, Cham, pp. 149–172. https://doi.org/10.1007/978-3-030-48457-6_9

Yáñez, A., Hassanzadeh-Kiabi, N., Ng, M.Y., Megías, J., Subramanian, A., Liu, G.Y., Underhill, D.M., Gil, M.L., Goodridge, H.S., 2013. Detection of a TLR2 agonist by hematopoietic stem and progenitor cells impacts the function of the macrophages they produce. Eur J Immunol 43, 2114–2125. https://doi.org/10.1002/eji.201343403

Yang, M., Shen, Z., Chen, D., Gan, H., Shen, Q., Yang, B., Du, X., 2012. Effects of 1,25-(OH)(2)D (3) on the expressions of vitamin D receptor, STAT5 and cytoskeletal rearrangement in human monocytes incubated with sera from type 2 diabetes patients and diabetic nephropathy patients with uremia. Inflamm Res 61, 511–520. https://doi.org/10.1007/s00011-012-0441-y

Yang, Z., Wara-Aswapati, N., Chen, C., Tsukada, J., Auron, P.E., 2000. NF-IL6 (C/EBPbeta) vigorously activates il1b gene expression via a Spi-1 (PU.1) protein-protein tether. J Biol Chem 275, 21272–21277. https://doi.org/10.1074/jbc.M000145200

Yoneyama, M., Kikuchi, M., Natsukawa, T., Shinobu, N., Imaizumi, T., Miyagishi, M., Taira, K., Akira, S., Fujita, T., 2004. The RNA helicase RIG-I has an essential function in double-stranded RNA-induced innate antiviral responses. Nat Immunol 5, 730–737. https://doi.org/10.1038/ni1087

Yoshida, A., Kato, J., Nakamae, I., Yoneda-Kato, N., 2013. COP1 targets C/EBPα for degradation and induces acute myeloid leukemia via Trib1. Blood 122, 1750–1760. https://doi.org/10.1182/blood-2012-12-476101

Yu, G., Wang, L.-G., Han, Y., He, Q.-Y., 2012. clusterProfiler: an R Package for Comparing Biological Themes Among Gene Clusters. Omics : a journal of integrative biology 16, 284–7. https://doi.org/10.1089/omi.2011.0118

Yunna, C., Mengru, H., Lei, W., Weidong, C., 2020. Macrophage M1/M2 polarization. Eur J Pharmacol 877, 173090. https://doi.org/10.1016/j.ejphar.2020.173090

Zanocco-Marani, T., Vignudelli, T., Gemelli, C., Pirondi, S., Testa, A., Montanari, M., Parenti, S., Tenedini, E., Grande, A., Ferrari, S., 2006. Tfe3 expression is closely associated to macrophage terminal differentiation of human hematopoietic myeloid precursors. Exp Cell Res 312, 4079–4089. https://doi.org/10.1016/j.yexcr.2006.09.015

Zanocco-Marani, T., Vignudelli, T., Parenti, S., Gemelli, C., Condorelli, F., Martello, A., Selmi, T., Grande, A., Ferrari, S., 2009. TFE3 transcription factor regulates the expression of MAFB during macrophage differentiation. Exp Cell Res 315, 1798–1808. https://doi.org/10.1016/j.yexcr.2009.03.018

Zarember, K.A., Godowski, P.J., 2002. Tissue expression of human Toll-like receptors and differential regulation of Toll-like receptor mRNAs in leukocytes in response to microbes, their products, and cytokines. J Immunol 168, 554–561. https://doi.org/10.4049/jimmunol.168.2.554

Zhang, D.E., Hetherington, C.J., Chen, H.M., Tenen, D.G., 1994. The macrophage transcription factor PU.1 directs tissue-specific expression of the macrophage colony-stimulating factor receptor. Mol Cell Biol 14, 373–381. https://doi.org/10.1128/mcb.14.1.373-381.1994

Zhang, P., Behre, G., Pan, J., Iwama, A., Wara-aswapati, N., Radomska, H.S., Auron, P.E., Tenen, D.G., Sun, Z., 1999. Negative cross-talk between hematopoietic regulators: GATA proteins repress PU.1. Proceedings of the National Academy of Sciences 96, 8705–8710. https://doi.org/10.1073/pnas.96.15.8705

Zhang, Z.H., Jhaveri, D.J., Marshall, V.M., Bauer, D.C., Edson, J., Narayanan, R.K., Robinson, G.J., Lundberg, A.E., Bartlett, P.F., Wray, N.R., Zhao, Q.-Y., 2014. A Comparative Study of Techniques for Differential Expression Analysis on RNA-Seq Data. PLOS ONE 9, e103207. https://doi.org/10.1371/journal.pone.0103207

Zhu, Y.P., Thomas, G.D., Hedrick, C.C., 2016. Transcriptional Control of Monocyte Development. Arterioscler Thromb Vasc Biol 36, 1722–1733. https://doi.org/10.1161/ATVBAHA.116.304054

Zizzo, G., Cohen, P.L., 2013. IL-17 Stimulates Differentiation of Human Anti-inflammatory Macrophages and Phagocytosis of Apoptotic Neutrophils in Response to IL-10 and Glucocorticoids. J Immunol 190, 5237–5246. https://doi.org/10.4049/jimmunol.1203017

Zizzo, G., Hilliard, B.A., Monestier, M., Cohen, P.L., 2012. Efficient clearance of early apoptotic cells by human macrophages requires M2c polarization and MerTK induction. J Immunol 189, 3508–3520. https://doi.org/10.4049/jimmunol.1200662